THE CHEMISTRY OF XENON[1]

JOHN G. MALM, HENRY SELIG,

Chemistry Division, Argonne National Laboratory, Argonne, Illinois

JOSHUA JORTNER, AND STUART A. RICE

Department of Chemistry and Institute for the Study of Metals, University of Chicago, Chicago, Illinois

CONTENTS

Table I

Equilibrium Constants for the Xenon-Fluorine System[a] (177)

Reaction	Temp., °K.					
	298.15	523.15	573.15	623.15	673.15	774.15
$Xe + F_2 = XeF_2$	1.23×10^{13}	8.79×10^4	1.02×10^4	1.67×10^3	3.59×10^2	29.8
$XeF_2 + F_2 = XeF_4$	1.37×10^{11}	1.43×10^3	1.55×10^2	27.2	4.86	0.50
$XeF_4 + F_2 = XeF_6$	8.6×10^5	0.944	0.211	0.0558	0.0182	0.0033

[a] *Italicized* values are calculated.

I. Introduction

A chemistry of xenon has developed only recently, beginning in the summer of 1962 when the fluorination of xenon was first demonstrated and stable fluorides of this element were first isolated. This review includes all of the experimental and theoretical work on this subject that has been published through June 1964. Publications after this date that have come to our attention have been included when the work has served to correct or elucidate earlier observations.

Although xenon has been shown to exhibit all the even valence states from II to VIII, and stable compounds of each of these have been isolated, xenon chemistry is limited to the stable fluorides and their complexes, two unstable oxides, and the aqueous species derived from the hydrolysis of the fluorides. While the chemistry of these compounds is well established, there remain many physical measurements to be made or to be repeated with greater precision. The novel nature of the subject has attracted many scientists to this field and resulted in some cases in the premature publication of inadequately established observations or speculations. In this regard, we have attempted to assess the reliability of some of the published results although, in some cases, the lack of experimental details made this difficult.

The chemistry of radon and krypton is even more restricted, being limited to the observations of their reaction with fluorine to form a compound or two. These studies are not reviewed here. The other noble gases, to date, remain inert, although several attempts have been made to predict their susceptibility to compound formation (118, 122, 125, 126, 171).

A number of short reviews (14, 33, 51, 53, 69, 72, 94, 119, 123, 141, 164) and a book (111) have appeared that briefly summarize the initial work on xenon chemistry, and the theory of binding in the xenon compounds has been recently authoritatively reviewed (43). A collection of individual papers, presented at a symposium at the Argonne National Laboratory in April 1963, has been published in the form of a book (71). Many of the papers contained in this book have since appeared in the open literature; and, in such cases, reference is made to the latter only.

II. The Xenon Fluorides

THE XENON-FLUORINE EQUILIBRIUM

The most thoroughly characterized compounds of xenon are the binary fluorides, probably because they are rather easily prepared. The fluorides are apparently formed in successive steps according to the following reactions (1, 176, 177).

$$Xe + F_2 \rightarrow XeF_2$$

$$XeF_2 + F_2 \rightarrow XeF_4$$

$$XeF_4 + F_2 \rightarrow XeF_6$$
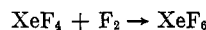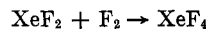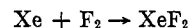
The proportions of the various fluorides present in a xenon-fluorine mixture are dictated by an appropriate set of equilibrium constants. These equilibrium constants, which have recently been determined in a careful study of the xenon-fluorine equilibrium system (177), are given in Table I. It should therefore now in principle be possible to prepare the three binary fluorides to a reasonable degree of purity by varying reaction conditions appropriately.

Although the equilibrium constants for the formation of the binary fluorides increase with lower temperatures, in the thermal method reaction products are observed only at temperatures exceeding 120° (46). Evidently it is necessary to establish a minimum concentration of fluorine atoms in order to obtain xenon fluorides. In fact, all preparative methods appear to require the production of fluorine atoms in the presence of xenon, and a variety of procedures have been devised to accomplish this. The only apparent exception to this rule is a report (89) that equimolar mixtures of xenon and fluorine at a total pressure of 30 atm. react at room temperature to form xenon difluoride.

Before the nature of the xenon-fluorine system was fully understood, a number of publications reported such physical properties as melting points, vapor pressures, and thermodynamic quantities for the binary fluorides. Subsequently, it became evident that these measurements were made on samples contaminated with one or more of the other fluorides or the oxyfluoride. Nearly all these observations, therefore, would bear repetition.

On the other hand, the molecular and crystal structures of these compounds, with the exception of the hexafluoride, are now well established.

1. XeF₂

a. Preparation

The existence of a lower fluoride of xenon was suggested in the initial report on XeF_4 (37). Subsequently, this lower fluoride was identified as XeF_2 (32, 67, 153, 160, 174). Since then XeF_2 has been prepared by a variety of methods, nearly all of which depend on the rapid removal of XeF_2 from the reaction system to prevent its further reaction resulting in the production of XeF_4.

Mixtures of xenon and fluorine have been circulated through a loop containing a section of nickel tubing heated to 400°, and an infrared monitoring cell to a U-tube maintained at −50° where the XeF_2 was condensed (153). The reaction is complete after 8 hr. This procedure has also been described in more detail accompanied by photographs and line diagrams (1, 155). Reaction products were observed at temperatures as low as 270° (1).

XeF_2 has also been prepared photochemically (174). Xe–F_2 mixtures were circulated through a nickel system with sapphire windows using a G.E. AH-6 high-pressure mercury arc for irradiation. Heating tape maintained at 90° on one leg of the loop and a −78° bath on the bottom U-bend assured circulation by convection and efficient removal of the XeF_2 from the reaction zone. With a ballast volume of appropriate size, this method has been scaled up to the production of 10-g. lots of XeF_2.

An electric discharge passed through Xe–F_2 mixtures has yielded XeF_2 at a rate of about 100 mg./hr. (67, 68). The XeF_2 was collected on a cold finger (−78°) which projected between the electrodes.

XeF_2 has been prepared in a flow system in 60–70% yields at temperatures of 250–400° using oxygen or air as carrier gas (47) and by irradiating mixtures of xenon and fluorine with high intensity Co^{60} γ-radiation (101) or electrons from a Van de Graaff accelerator (95, 102).

Small amounts of XeF_2 have also been prepared without the use of elemental fluorine. One method employed passage of an electric discharge through mixtures of xenon and CF_4, or xenon and SiF_4, in a refrigerated flow system (110). Yields of 50–150 mg. were obtained within 1–2 hr.

XeF_2 has been obtained by heating mixtures of Xe with CF_3OF at pressures of 250 atm. and 500°K. or xenon with FSO_3F at 150 atm. and 450°K. (55). In the latter case, measurable amounts of XeF_4 were formed as well.

XeF_2 has been prepared in nonisolable amounts by the matrix isolation method (165) using ultraviolet irradiation of Xe–F_2 mixtures deposited on CsI windows at 20°K.

From a practical standpoint, of the listed methods only the first two (153, 174) promise to be useful for preparative purposes, the remainder being more or less exotic variations based on the same principles. Even the most useful of preparative techniques (153, 174) require the construction of somewhat elaborate circulating systems to remove XeF_2 from the reaction zones in order to prevent formation of XeF_4. A method more generally useful may be the reaction of XeF_4 (or fluorine) with excess xenon at high pressure according to the reaction

$$XeF_4 + Xe \rightarrow 2XeF_2$$
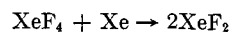
The calculated equilibrium constant for this reaction is ⌐100 at 300° (177).

b. Physical Properties

Xenon difluoride is a colorless solid which is stable at room temperature (174). The vapor is colorless and possesses a penetrating, nauseating odor (68). The vapor pressure is several millimeters at room temperature, and XeF_2 can be handled readily in a vacuum system. It sublimes easily and grows into large transparent crystals. Although data on the chemical properties are scarce, the crystal structure and vibrational spectrum are well characterized. Physical data are collected in Table II.

c. Stability

Xenon difluoride is stable provided it is dry and free of contaminants. It can be kept indefinitely in nickel containers; and despite reports to the contrary (68), XeF_2 can be stored in thoroughly dried glass vessels.

d. Chemical Properties

Studies of the chemical properties of XeF_2 are limited to a few isolated reactions. The compound behaves as a mild fluorinating agent. From qualitative observations (68), XeF_2 reacts slowly with water, dilute NaOH, dilute H_2SO_4, and kerosene. With methanol, XeF_2 reacts more strongly. XeF_2 liberates iodine from acidified KI solutions.

The hydrolysis of cold XeF_2 with 1 M NaOH results in a yellow color which disappears rapidly upon warming above 0° (108b), while xenon and oxygen are liberated quantitatively according to the reaction

$$XeF_2 + H_2O \rightarrow Xe + 0.5O_2 + 2HF$$
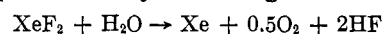
leaving a colorless solution behind.

XeF_2 reacts with fluorine to produce XeF_4 (1, 176, 177) according to

$$XeF_2 + F_2 \rightarrow XeF_4$$
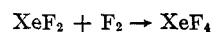
The rate of this reaction increases as the partial pressures of XeF_2 and F_2 are increased and as the temperatures is raised (1). The equilibrium constants for the production of XeF_2 and XeF_4 from the elements have been measured (177).

TABLE II

PHYSICAL PROPERTIES OF XeF_2

Appearance   **Ref.**

Colorless crystals and colorless vapor at room temperature   68, 174

Molecular structure

Linear, symmetric, triatomic molecule; symmetry group $D_{\infty h}$ 153

Molecular constants

		Ref.
Xe–F distance ~ 1.9 Å. (calculated from P–R separation of infrared band)		152
Xe–F stretching constant	2.85 mdynes/Å	1, 153
Interaction force constant	0.11 mdyne/Å.	153
Bending constant	0.19 mdyne/Å.	1

Vibrational spectrum bands

Frequency, cm.$^{-1}$	Assignment	Relative intensity	
Raman (solid)			
108		0.33	
497	ν_1	1.00	1, 110, 152, 153, 174
Infrared (vapor)			
213.2	ν_2	vs	
555 $\begin{array}{l}566\ R\\550\ P\end{array}$	ν_3	vs	
1070	$\nu_1 + \nu_3$	w	
Infrared (solid) at 20°K.			
510	ν_1	Forbidden	165
547	ν_3		

Ultraviolet absorption in the gas phase   86

Wave length, Å.	Half-width, cm.$^{-1}$	Estd. extinction coeff., l. mole^{-1} cm.$^{-2}$	Estd. oscillator strength, f.
2300	8249	0.86×10^2	0.0033
1580	8060	1.12×10^4	0.42
1425	(1000)	0.4×10^4	0.02
1335	(1290)	0.4×10^4	0.02
1215	(2070)	0.4×10^4	0.03
1145	(2730)	0.6×10^4	0.06

Melting point

140° (can supercool 50°)   1

Vapor pressure

		Ref.
25°	3.8 mm.	1
100°	318 mm.	

Solubility in anhydrous HF

Temp., °C.	Solubility, moles/1000 g.
−2.0	6.38
12.25	7.82
29.95	9.88

Solutions do not conduct

Solubility in water   9

25 g./l. at 0°

Magnetic susceptibility   68

$-\chi_M = 40\text{--}50 \times 10^{-6}$ e.m.u.

Crystallographic data

Tetragonal body-centered lattice   145

$a = 4.315 \pm 0.003$ Å.

$c = 6.990 \pm 0.004$ Å.

Space group I4/mmm

Xe–F distance	2.14 ± 0.14 Å. (X-ray)	145
	2.00 ± 0.01 Å. (neutron diffraction)	97

Density of solid

4.32 g./cm.^{3} calculated from X-ray data   145

Relative abundances and appearance potentials of ions in mass spectra   161

Ion	Abundance	Appearance potential, e.v.
XeF_2^+	47	12.6 ± 0.1
XeF^+	100	13.3 ± 0.1
Xe^+		12.0 ± 0.1

TABLE II (*Continued*)

Ref.

Heat of formation

$\Delta H_f(g) = -25.9$ kcal. mole^{-1} at 25° (calculated from equilibrium constant   177
and entropy from spectroscopic data)   176
$\Delta H_f(g) = -37 \pm 10$ kcal. mole^{-1} at 150° (from mass spectra appearance potentials)   161

Heat of sublimation

$\Delta H_{subl} = 12.3 \pm 0.2$ kcal. mole^{-1} (from temperature dependence of 1750-Å. band in the spectra)   84

Bond energy

$E_{Xe-F} = 31.3$ kcal. mole^{-1} 176, 177
$E_{Xe-F} = \sim39 \pm 10$ kcal. mole^{-1} 161

Hydrogen reduces (174) XeF$_2$ at 400° according to

$$XeF_2 + H_2 \rightarrow Xe + 2HF$$
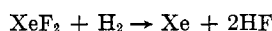
This reaction has been used as an analytical tool for the determination of XeF$_2$ (174).

SO$_3$ reacts with XeF$_2$ (55) at 300° to liberate Xe, O$_2$, and S$_2$O$_5$F$_2$.

XeF$_2$ reacts with SbF$_5$ (47) to give an adduct of composition XeF$_2\cdot$2SbF$_5$.

e. Photochemistry

One of the first methods of producing XeF$_2$ in larger quantities was by a photochemical reaction (174). The effect of various parameters on the yields has been investigated further in attempts to elucidate the reaction mechanism (175). The mechanism appears to be extremely complex and only the following qualitative observations have been made:

(1) Atomic fluorine is produced by light absorption in the fluorine 3000-Å. absorption band (170).

(2) The quantum yield for 1:1 mixtures of Xe and F$_2$ decreases with increasing pressure.

(3) At a total pressure of 1000 mm., a limiting quantum yield of 0.3 is reached, and no changes in quantum yield with intensity are observed.

(4) For a given Xe pressure, increasing the F$_2$ pressure decreases the quantum yield.

(5) For low F$_2$ pressures, increasing the Xe pressure decreases the quantum yield.

(6) At high F$_2$ pressures, increasing the Xe pressure slightly increases the quantum yield.

f. Methods of Analysis

The existence of XeF$_2$ as an independent species was first observed in the mass spectrometric analyses of reaction products from heated xenon–fluorine mixtures (160). This method has proved to be a valuable qualitative tool for the detection of XeF$_2$, as well as ascertaining the absence of XeF$_4$ in such samples (68, 105, 110, 160, 174). Under optimum conditions, as little as 0.1% of XeF$_4$ in XeF$_2$ can be detected by this method.

Another method for checking the purity of XeF$_2$ involves the use of infrared spectroscopy (153, 174). The absence of an absorption band at 590 cm.$^{-1}$ in an infrared spectrum obtained at room temperature sets an upper limit of about 1% to the amount of XeF$_4$ present.

Quantitative analyses of XeF$_2$ have been performed by reaction with hydrogen at 400° (174). The resulting Xe and HF are separated and weighed (37).

Another method (108b) consists of hydrolyzing the cold XeF$_2$ with 1 M NaOH, collecting the xenon and oxygen with a Toepler pump, and measuring the pressure. The proportions of xenon and oxygen may be determined with a mass spectrometer. Fluoride can be determined separately.

2. XeF$_4$

a. Preparation

Xenon tetrafluoride, the first simple compound of xenon to be synthesized (37), was prepared by heating mixtures of xenon and fluorine in a 1:5 ratio at 400° and about 6 atm. in a sealed nickel can. Yields were essentially quantitative. Half-gram samples of XeF$_4$, relatively free of XeF$_2$ and XeF$_6$, were obtained by this procedure. This method can be easily scaled up by using larger vessels provided the same reaction conditions are maintained.

Flow methods have been used (66, 162) to prepare XeF$_4$. By diffusing Xe into a stream of fluorine through a nickel tube at dull red heat, a 30–50% yield of XeF$_4$ has been obtained (66). In an adaptation of this method, XeF$_4$ was produced when a 4:1 molar ratio of F$_2$ and xenon was passed through a nickel tube at 300° (162). With a residence time of 1 min. in the heated zone, the yield was 100%.

Essentially quantitative yields of XeF$_4$ have been reported for the electric discharge method (92). A stoichiometric mixture of xenon and fluorine was fed into a Pyrex reaction vessel cooled to −78°. Yields of about 1.5 g. in 3.5 hr. were obtained.

Some of the advantages claimed for this method are outweighed by the complexity of the required apparatus.

XeF$_4$ has been reported to form when Xe–F$_2$ mixtures are circulated through a nickel oven at 560° into a trap held at 0°. Up to 11 g./hr. was produced in 97% yield (138). No analyses were given of this preparation. Some of the chemical properties for the

TABLE III

PHYSICAL PROPERTIES OF XeF$_4$

Ref.

Appearance
    Colorless crystals and colorless vapor at room temperature   37
Molecular structure
    Symmetrical square-planar molecule; symmetry group D$_{4h}$ 20, 39
Molecular constants
    Xe–F distance 1.85 ± 0.2 Å. From P–R separation in the infrared spectrum   39
                1.94 ± 0.01 Å.   Electron diffraction   20
    Xe–F stretching constant   3.00 mdynes/Å.   39
       Interaction force constant between bonds at right angles   0.12 mdyne/Å.   39
Vibrational spectrum bands

Frequency, cm.$^{-1}$	Assignment	Relative intensity	
Raman (solid)			
543	ν_1	vs	39
235	ν_3	w	
502	ν_5	vs	
Infrared (vapor)			
586 $\begin{smallmatrix}581\ P\\591\ R\end{smallmatrix}$	ν_6	vs	
291	ν_2	s	
(123^a)	(ν_7)	w	
1105	$\nu_5 + \nu_6$	w	
1136	$\nu_1 + \nu_6$	w	
Infrared (solid)			
290	ν_2		165
568	ν_6		
Raman (in anhydrous HF)			
550–553	ν_1		73

Ultraviolet absorption spectrum in the gas phase   86, 131

Wave length, Å.	Half-width, cm.$^{-1}$	Estd. extinction coeff., l. mole^{-1} cm.$^{-2}$	Estd. oscillator strength, f.
2280		398	0.009
2580	7,000	160	0.003
1840	10,000	4.75 × 10^3	0.22
1325	11,200	1.5 × 10^4	0.80

Melting point
    ~114°   34
Vapor pressure
    ~3 mm. at 20°   37
Solubility in anhydrous HF   73

Temp., °C.	Solubility, moles/1000 g.
20	0.18
27	0.26
40	0.44
60	0.73

Solution does not conduct

Magnetic susceptibility
    χ_M = −50.6 × 10^{-6} e.m.u. at room temperature   149
        = −(52 ± 3) × 10^{-6} e.m.u. between 77 and 293°K. (estimated from graph)   104
Crystallographic data
    Monoclinic, space group C$_{2n}^5$-P2$_1$/n   74, 145, 162
       a = 5.03 ± 0.03, b = 5.90 ± 0.03, c = 5.75 ± 0.03 Å., β = 100 ± 1°
       a = 5.03, b = 5.92, c = 5.79 Å., β = 99°27'   145
       a = 5.050, b = 5.922, c = 5.771 Å., β = 99.6 ± 0.1°   162
    Xe–F distance   1.92 ± 0.03 Å.   74
                         1.91 ± 0.02   162
                         1.953 ± 0.002 (neutron diffraction)   31
    F–Xe–F angle   86 ± 3°   74
                         90.4 ± 0.9   162
                         90.0 ± 0.1 (neutron diffraction)   74
Density of solid
    4.04 g./cm.^{3} (calculated from X-ray data if 2 molecules/unit cell)   145, 162
    4.10 g./cm.^{3} 74

TABLE III (Continued)

Relative abundances and appearance potentials of ions in mass spectra			105,161
Ion	Abundance	Appearance potential, e.v.	
$Xe_2F_5^+$		13.8 ± 0.2	
XeF_4^+	7	12.9 ± 0.1	
XeF_3^+	100	13.1 ± 0.1	
XeF_2^+	60	14.9 ± 0.1	161
XeF^+	67	13.3 ± 0.1	
Xe^+	800	12.4 ± 0.1	

Heat of formation

$\Delta H_f(g) = -57.6^b$ kcal. mole^{-1} (at 120° from heat of reaction $XeF_4(g) + 2H_2(g) = Xe(g) + 4HF(g)$) 157

$\Delta H_f(g) = -48^b$ kcal. mole^{-1} (at 25° from heat of reaction $XeF_4(s) + 4I^- = Xe + I_2 + 4F^-$ and heat of sublimation 59

$\Delta H_f(g) = -51.5$ kcal. mole^{-1} (at 25° from $Xe-F_2$ equilibria) 177

$\Delta H_f(g) = -53 \pm 5$ kcal. mole^{-1} (at 150° from mass spectra appearance potentials) 161

Heat of sublimation

$\Delta H_{subl} = 15.3 \pm 0.2$ kcal. mole^{-1} (from ultraviolet spectroscopy between -15 and 22°) 84

Bond energy

$E_{Xe-F} = 32.8^b$ kcal. mole^{-1} 157

$\sim$30 kcal. mole^{-1} 59

$\sim$32 $\pm$ 2 kcal. mole^{-1} 161

$C_p°_{298.16}$ (sat.) $= 28.334$ cal. mole^{-1} 82

$\Delta S_f°_{298} = -102.5$ cal. mole^{-1} deg.$^{-1}$ (from heat capacity) 82

$\Delta F°_{298} = -29.4$ kcal. mole^{-1} (using $\Delta H° = -60$ kcal. mole^{-1} which is uncertain) 82

$S°_{298.16} = 35.0 \pm 1.0$ e.u. 82

Debye temperature $\theta = 122°$ (uncertain due to contributions from intramolecular vibrations)

^{a} This has since been ascribed to HF impurity. ^{b} Recalculated using recent value for heat of formation of HF (50).

product seem more characteristic of XeF_2 than of XeF_4.

XeF_4 has been prepared in nonisolable quantities by prolonged ultraviolet irradiation of solid $Xe-F_2$ mixtures deposited on CsI windows at 20°K. (165).

b. Physical Properties

XeF_4 is a colorless solid which is stable at room temperature (37). The vapor pressure at room temperature is about 3 mm. The vapor is colorless. XeF_4 sublimes easily to form large colorless crystals. The melting point is about 114° (34). As in the case XeF_2, chemical properties of XeF_4 are not well known, but its crystal structure and molecular structure are well established (20, 31, 39, 74, 145, 162). XeF_4 is only sparingly soluble in anhydrous HF (73) and insoluble in n-C_7F_{16} (37). Physical properties of XeF_4 are given in Table III.

c. Stability

Xenon tetrafluoride is stable when pure and free of moisture. It can be kept indefinitely in nickel or monel containers. Despite reports to the contrary (138), XeF_4 (free of moisture and HF) can be stored indefinitely in glass vessels (37).

d. Chemical Properties

As in the case of XeF_2, studies of chemical properties of XeF_4 are thus far limited to a few isolated observations. XeF_4 is a moderately strong fluorinating agent comparable in reactivity to UF_6 (32). Dissolved in anhydrous HF, XeF_4 fluorinates bright platinum to PtF_4, releasing Xe gas (32, 138).

XeF_4 is reported to be insoluble in and inert to CCl_4, CS_2, $HCON(CH_3)_2$, $(C_2H_5)_2O$, and cyclohexane (138). Contrary to this observation, it has been reported that XeF_4 dissolved in diethyl ether with gas evolution to give a strongly oxidizing solution (48). The latter observation is more likely to be correct.

XeF_4 is said to react strongly with tetrahydrofuran, dioxane, and ethanol (138). It reacts also with acetic acid, concentrated HNO_3, and H_2SO_4 (138).

At room temperature XeF_4 does not react with hydrogen, but at 70° a slow reaction sets in which goes rapidly to completion at 130° (157). The reaction of XeF_4 with hydrogen at 400° has been used as an analytical method for determination of XeF_4 (37).

XeF_4 reacts with a large excess of xenon at 400° to form XeF_2 (37). With a large excess of fluorine, XeF_4 reacts at 300° to form XeF_6 (177). XeF_4 is also reported to react with O_2F_2 between 140 and 195°K. to give XeF_6 and oxygen (159). SF_4 reacts with XeF_4 to produce Xe and SF_6. The reaction is slow at 23° and only 20% complete after 20 hr. (159).

No reaction occurs between XeF_4 and BF_3 up to 200° (47). A violet solid, stable below $-100°$, reported earlier for a mixture of XeF_4 and BF_3 (138) has since been ascribed to impurities. XeF_4 does not combine with NaF or KF (47).

XeF_4 dissolves with gas evolution in liquid SbF_5 to give a greenish solution from which the compound $XeF_2 \cdot 2SbF_5$ is readily isolated (47). With TaF_5, the complex $XeF_2 \cdot TaF_5$ is formed (47).

The hydrolysis of XeF_4 is the most thoroughly investigated reaction of this compound (8, 108b, 178).

Upon hydrolysis, only a portion of the xenon is liberated as the gas. A large fraction remains in solution as a molecular species (8, 108b, 178). The over-all stoichiometry in water, dilute acid, or dilute base is given by the equation (108b)

$$XeF_4 + 2H_2O \rightarrow \text{2/3}Xe + \text{1/2}O_2 + \text{1/3}XeO_3 + 4HF$$
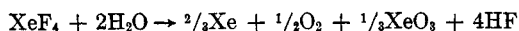
XeF$_4$ reacts with acetic anhydride with strong gas evolution. After removal of excess anhydride, a white solid containing the anhydrides of succinic and glutamic acids remains behind (75).

XeF$_4$ dissolves in $(CF_3CO)_2O$ without reaction. If the solution is treated with trifluoroacetic acid, and subsequently the excess is sublimed off at $-40°$, a bright yellow unstable solid remains. The mass spectrum of this solid shows fragments corresponding to $XeFCO_2^+$, $XeFCO^+$, and $XeCO^+$, in addition to the xenon fluoride fragments. On the basis of the similarity of this mass spectrum with those obtained with silicon tetraacetate and iodine tritrifluoroacetate, it has been assumed that the substance is xenon tetratrifluoroacetate (75).

e. Radiation Chemistry

Irradiation of XeF$_4$ with 420 Mrads of Co^{60} γ-radiation at $45°$ causes some decomposition to the elements (102). The increase in pressure fits the empirical equation $p = 0.47t^{0.58}$, where p is in millimeters and t is in minutes.

f. Methods of Analysis

Contaminants most likely to be present in XeF$_4$ are XeF$_2$ and XeF$_6$.

Infrared spectra taken at room temperature give about the same sensitivity as previously quoted for XeF$_2$ (1%), but XeF$_6$ can be detected in amounts as little as 0.2%. XeF$_6$, as a rule, does not present any difficulties. Because of its greater volatility, it can be removed by flashing off several equilibrium vapor pressure heads. Small amounts of XeF$_2$ can also be removed by pumping away several equilibrium vapor pressure heads.

Quantitative analyses for XeF$_4$ have been performed by reaction with hydrogen (37). Alternatively, XeF$_4$ has been treated with mercury (92) according to the reaction

$$XeF_4 + 4Hg \rightarrow Xe + 2Hg_2F_2 \text{ (or } 2HgF_2)$$
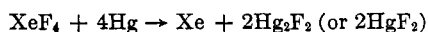
The Xe pressure is measured, and fluorine is determined by the weight increase of the mercury.

XeF$_4$ can also be determined by reaction with KI solution (66) according to

$$XeF_4 + 4I^- \rightarrow Xe + 2I_2 + 4F^-$$

Again, the Xe pressure is determined and the amount of liberated iodine measured by titration.

3. XeF$_2$·XeF$_4$

Xenon difluoride and xenon tetrafluoride have been found to form a 1:1 molecular addition compound (30). This phase had earlier been thought to correspond to a high density phase of XeF$_4$ (29, 145).

Crystals of XeF$_2$·XeF$_4$ were prepared by controlled mixing of XeF$_2$ and XeF$_4$ vapors (30). These crystallize in a monoclinic phase with $a = 6.64 \pm 0.01$, $b = 7.33 \pm 0.01$, $c = 6.40 \pm 0.01$ Å., and $\beta = 92° 40' \pm 5'$ (29). The probable space group is P2$_1$/c. The calculated density is 4.02 g./cm.^{3} (30). The XeF$_4$ and XeF$_2$ units essentially preserve their identity in the structure. There are no unusually short distances between these units, so that apparently only weak bonds hold the molecules together.

4. XeF$_6$

a. Preparation

Xenon hexafluoride was first prepared independently at a number of laboratories (46, 108a, 150, 172). Nickel or monel high pressure reaction vessels are used. In general, greater than 95% conversion to XeF$_6$ is obtained with F$_2$–Xe ratios of 20:1 at 50 atm. pressure. Reaction between Xe and F$_2$ begins at temperatures as low as $127°$, and rapid reaction occurs at $210-250°$. Pressure–temperature studies suggest that at $400°$ XeF$_4$ would be the dominant species present (46).

At $700°$ and about 200 atm., essentially quantitative conversion to XeF$_6$ occurs (150). The equilibrium mixture obtained must correspond to that prevailing at a lower temperature since no quenching procedure was used.

Mass spectrographic analyses of purified samples show the presence of XeF$_6^+$ and its fragmentation products (108a).

In a variation of the other methods (172), F$_2$ and Xe were caused to react in a stainless steel container which was kept at $-115°$ or at $80°$. The reaction was initiated by an internal electric heater made of nickel gauze maintained at $350-450°$. Mixtures of XeF$_6$ and lower fluorides were obtained.

XeF$_6$ has been obtained in an electrical discharge apparatus (159). A 3:1 F$_2$ to Xe mixture was used and the product trapped at $-78°$. Under the same conditions, but with 2:1 F$_2$ and Xe ratios, XeF$_4$ is produced. This would suggest that it might be difficult to control this reaction to give a single product.

XeF$_4$ (159) reacts with O$_2$F$_2$ between $-133°$ and $-78°$ to produce XeF$_6$.

XeF$_6$ can be freed of the more common volatile impurities (HF, BF$_3$, SiF$_4$) by pumping at $-78°$, in the same manner that the volatile metal hexafluorides are purified. Depending on the conditions of preparation, the XeF$_6$ product will be more or less

Table IV

Physical Properties of XeF_6

Ref.

Appearance
   Solid, colorless below 42°; yellow above 42°   108a, 172
   Vapor, yellow
   Liquid, yellow
Melting point
   46°
Vapor pressure

Temp., °C.	0	0.04	9.78	18.10	20	22.67	
Pressure, mm.		2.70	7.11	15.10		23.43	177
Pressure, mm.	3				20		155

Heat of sublimation
   $\Delta H_{subl} = 15.3$ kcal. mole^{-1} (calculated from vapor pressure data)   177
Vibrational spectrum bands

	Frequency, cm.$^{-1}$	Relative intensity	
Infrared (vapor)			152
	520	m	
	612	s	
	1100	w	
	1230	w	
Raman (solid)			152
	582	4	
	635	8	
	655	10	

Ultraviolet absorption spectrum (vapor)
   3300 Å. (s), half-width ~580 Å., very intense absorption below 2750 Å.   108a
Solubility in anhydrous HF   73

Temp., °C.	Solubility, moles/1000 g.
15.8	3.16
21.7	6.06
28.5	11.2
30.25	19.45

Electrical conductivity in anhydrous HF (0°)   73

Concn., mole/l.	Specific conductivity, ohm^{-1} cm.$^{-1}$	Molar conductivity, ohm^{-1} cm.^{2}
0.02	3.52×10^{-3}	147
0.07	8.44	126
0.09	13.4	150
0.14	15.0	110
0.16	16.7	102
0.18	19.2	110
0.24	23.0	96
0.49	33.6	69
0.75	44.9	60

Heat of formation
   $\Delta H_f(g) = -82.9^a$ kcal. mole^{-1} at 120° (obtained from heat of reaction: $XeF_6(g) + 3H_2(g) \rightarrow Xe(g) + 6HF(g)$)   157
Bond energy
   ~32.3^a kcal. mole^{-1} 157

^{a} Recalculated using recent value for heat of formation of HF (50).

contaminated with XeF_4 (and possibly XeF_2). The reaction of XeF_6 with glass or with traces of H_2O gives rise to $XeOF_4$ impurity.

Infrared spectroscopy offers one method of analysis. However, the XeF_4 band appears as a shoulder on the broad 612-cm.$^{-1}$ XeF_6 band, and, therefore, poor sensitivity is obtained (3–4%). The absence of an absorption at 928 cm.$^{-1}$ in an infrared scan obtained at room temperature sets an upper limit of about 1% to the amount of $XeOF_4$ present.

Chemical analysis for F^- does not offer a sensitive method for the detection of these impurities. Perhaps the most sensitive method for the detection of small amounts of XeF_4 in XeF_6 would be to take advantage of the different manner in which these compounds behave on hydrolysis (8).

The vapor pressures of these compounds are such that it is very difficult to effect any separation; however, with $XeOF_4$ some separation from XeF_6 can be obtained (176).

b. Physical Properties

The physical properties of XeF$_6$ are given in Table IV. The structures of the solid and the vapor species of XeF$_6$ are unknown.

The rate of exchange of F^{18} between fluorine gas and xenon hexafluoride has been studied at 150° (142). The rate of exchange was found to be a linear function of fluorine concentration. This has been explained in terms of an associative mechanism.

c. Chemical Properties

XeF$_6$ is a stable compound and can be stored indefinitely in nickel containers. However, it reacts rapidly with quartz (36, 155) to give rise to XeOF$_4$; reaction with CaO gives the same product. The reaction of XeF$_6$ with small amounts of water produces XeOF$_4$, which will appear as an impurity in most XeF$_6$ samples unless it is handled in completely dry equipment.

Further reaction with water produces the explosive XeO$_3$. However, if the hydrolysis is carried out slowly at low temperature with large excess of H$_2$O, the XeF$_6$ may be quantitatively converted to an aqueous solution of XeO$_3$.

XeF$_6$ reacts with BF$_3$ and AsF$_5$ at room temperature to form the 1:1 addition compounds XeF$_6$·BF$_3$ and XeF$_6$·AsF$_5$ (140).
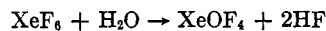
Hydrogen reacts violently with XeF$_6$ to give Xe and HF. XeF$_6$ reacts with mercury to give xenon and mercury fluoride. This reaction has been used for the analytical determination of XeF$_6$ (172). XeF$_6$ forms an addition compound of unknown composition with NaF (143).

5. XeOF$_4$

The existence of XeOF$_4$ as an independent species was first suggested (160) from observations of XeOF$_4$$^+$ ions as minor contaminants in XeF$_4$ samples. The compound has since been prepared in weighable amounts.

a. Preparation

XeOF$_4$ has been prepared by the partial hydrolysis of XeF$_6$ according to the reaction

$$XeF_6 + H_2O \rightarrow XeOF_4 + 2HF$$

Smith (156) prepared the compound in the same circulating loop which was used to prepare XeF$_2$ (153), with omission of the heating zone. With XeF$_6$ present in the loop at its room temperature vapor pressure, air saturated with water was admitted while circulation continued. The reaction was followed by monitoring the disappearance of the 520-cm.$^{-1}$ band of XeF$_6$. Yields of XeOF$_4$ were as large as 80%.

Based on the same reaction, XeOF$_4$ was prepared in a static system (36) by condensing stoichiometric

quantities of XeF$_6$ and H$_2$O into a large nickel container and allowing the container to warm to room temperature. The amounts of material taken were such that the XeF$_6$ and H$_2$O would be completely vaporized at room temperature.

Another method of preparation, although not suitable for larger quantities (155), is based on the reaction of XeF$_6$ with silica (36, 155). XeF$_6$ is sealed in a silica

$$2XeF_6 + SiO_2 \rightarrow 2XeOF_4 + SiF_4$$

flask fitted with a break-seal and heated to 50° until the characteristic yellow color of XeF$_6$ vapor disappears. The bulb is then cooled with Dry Ice and the SiF$_4$ pumped off. The products should be removed soon after the XeF$_6$ is consumed to avoid further reaction resulting in formation of the explosive XeO$_3$.
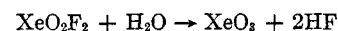
b. Physical Properties

XeOF$_4$ is a colorless liquid at room temperature and is somewhat more volatile than XeF$_6$. A plot of the vapor pressure $vs.$ $1/T$ has been given by Smith (155), based on the relative absorbance of an infrared band as a function of temperature in conjunction with the determination of the absolute vapor pressure at several temperatures. Since the latter have not yet been measured precisely, this plot must be considered provisional. Although the molecular structure of XeOF$_4$ has been determined, the physical properties are not yet well established as shown by the disparity in reported data. The vapor pressures and melting point data can at best be considered qualitative. The physical properties of XeOF$_4$ are given in Table V.

c. Stability

XeOF$_4$ appears to be stable and can be stored indefinitely in nickel containers (36). It is slightly less reactive than XeF$_6$ and apparently attacks quartz more slowly (155). XeOF$_4$ reacts slowly with polyethylene at room temperature (155).

d. Chemical Properties

XeOF$_4$ reacts with water, ultimately resulting in the formation of XeO$_3$ (36, 156). Traces of XeO$_2$F$_2$ have been found in mass spectrometric analyses of XeOF$_4$. Hence, the hydrolysis probably proceeds stepwise (36) according to the reactions

$$XeOF_4 + H_2O \rightarrow XeO_2F_2 + 2HF$$

$$XeO_2F_2 + H_2O \rightarrow XeO_3 + 2HF$$

Xenon oxytetrafluoride reacts with hydrogen at 300°, the following reaction taking place (36).

$$XeOF_4 + 3H_2 \rightarrow Xe + H_2O + 4HF$$

This reaction has been used as a method of analysis (36).

TABLE V

PHYSICAL PROPERTIES OF XeOF$_4$

Ref.

Appearance
  Colorless liquid and colorless vapor at room temperature   36, 156
Molecular structure
  Square pyramid with Xe close to the plane of the four fluorine atoms and oxygen at the apex.   Symmetry group C$_{4v}$ 38, 156
Molecular constants
  Xe–F stretching constant, 3.21 mdynes/Å.   156
  Xe–O stretching constant, 7.11 mdynes/Å.   156
Vibrational spectrum bands

	Assignment	Frequency	Relative intensity	
Infrared spectrum (vapor)				
	$\nu_1(A_1)$	928.2, 926	s, s	38, 156
	$\nu_2(A_1)$	578, 576	vw, m	
	$\nu_3(A_1)$	288, 294	s, s	
	$\nu_7(E_u)$	609, 608	vs, vvs	
	$\nu_8(E_u)$	362, 361	ms, s	
	$\nu_2 + \nu_7$	1186	w	38
	$2\nu_2$	1156	w	38
	$2\nu_8$	735	vw	38
Raman spectrum (liquid)				
	$\nu_1(A_1)$	919, 920	s, p; 20P	38, 156
	$\nu_2(A_1)$	566, 567	vs, p; 100P	
	$\nu_3(A_1)$	286, 285	vw; 2P	
	$\nu_4(B_1)$	530, 527	w; 40D	
	$\nu_5(B_1)$	231, 233	s; 6D	
	$\nu_8(E_u)$	364, 365	mw; 15D	
	$\nu_9(E_u)$	161	3D	156
	$\nu_2 + \nu_5$	818	vw	38

Melting point
  −28°   36
  −41°   156
Vapor pressure
  0°   7.0 mm.   156
  8 mm.   36
  23°   29 mm.

III. COMPLEXES OF XENON

A. Xe(PtF$_6$)$_x$

1. General

Xenon was first reported to participate in chemical reactions in June 1962 (11). According to this report, tensimetric titration of xenon with PtF$_6$ at room temperature resulted in formation of XePtF$_6$. Subsequent work (12) has indicated that the stoichiometry is much more complex and that compounds of the type Xe(PtF$_6$)$_x$ are formed where x lies between 1 and 2. It has been suggested that these compounds may be double salts of xenon fluorides and lower valent platinum fluorides (54). The issue is clouded further by the possibility of side reactions (32) in which xenon is fluorinated by PtF$_6$ to form simple fluorides. Moreover, the products may have been contaminated by lower fluorides of platinum formed from decomposition of the very reactive and unstable platinum hexafluoride.

Combustion of a platinum wire in a xenon–fluorine atmosphere was reported to result in the formation of XePtF$_6$ (106). Hydrolysis of this compound,

however, resulted in an equimolar mixture of xenon and oxygen contrary to the expected 2:1 ratio. More careful experiments showed that the compound obtained is actually XePt$_2$F$_{12}$ (107).

The initial interest in this first chemical reaction of xenon has been supplanted by the intensive studies of the simple binary fluorides subsequently discovered. Consequently, the nature of these complexes is as yet poorly understood.

Studies with other hexafluorides (12, 32) indicate that those which are thermodynamically unstable (PtF$_6$, RuF$_6$, RhF$_6$, PuF$_6$) react with xenon at room temperature, while stable hexafluorides (e.g., UF$_6$, NpF$_6$, IrF$_6$) do not react under ordinary conditions.

2. Physical Properties (12)

Xe(PtF$_6$)$_x$ is yellow as a thin film, but deep red in bulk. It has negligible vapor pressure at room temperature but can be sublimed in vacuo when heated. The solid becomes glassy at 115° but does not melt below its decomposition temperature of 165°.

Xe(PtF$_6$)$_x$ is insoluble in CCl$_4$. The infrared spectrum of the solid ($x = 1.72$) exhibits absorptions at

652 cm.$^{-1}$ (vs) and 550 cm.$^{-1}$ (s) close to those obtained for KPtF$_6$ and O$_2$PtF$_6$.

3. Chemical Properties (12)

At 165°, Xe(PtF$_6$)$_x$ $(x = 1.8)$ is reported to decompose to XeF$_4$ and a brick-red solid of composition XePt$_2$F$_{10}$ (105).

Xe(PtF$_6$)$_x$ reacts with RbF or CsF in liquid IF$_5$ to form salts which have been identified as RbPtF$_6$ and CsPtF$_6$, respectively, on the basis of their X-ray diffraction patterns.

These reactions in conjunction with the infrared data have been adduced as evidence for pentavalent platinum in Xe(PtF$_6$)$_x$.

Heating Xe(PtF$_6$)$_{1.89}$ at 130° with sufficient Xe to produce the 1:1 complex results in changing x to 1.29. Prolonged heating with excess xenon results in no further change.

The hydrolysis of Xe(PtF$_6$)$_x$ $(x = 1)$, is said to proceed according to the reaction (11)

$$XePtF_6 + 3H_2O \rightarrow Xe + 0.5O_2 + PtO_2 + 6HF$$

while the hydrolysis of Xe(PtF$_6$)$_x$ $(x = 2)$, follows the reaction (107)

$$Xe(PtF_6)_2 + 6H_2O \rightarrow Xe + O_2 + 2PtO_2 + 12HF$$

B. Other Metal Hexafluoride Complexes

A chemical reaction between Xe and RuF$_6$ at room temperature has been reported to form Xe(RuF$_6$)$_x$ where x ranges between 2 and 3 (32). A deep red adduct of formula Xe(RhF$_6$)$_{1.10}$ has also been reported (12) to form by combination of xenon and rhodium hexafluoride at room temperature.

Xenon is also supposed to form adducts with PuF$_6$ (32).

C. Xenon Difluoride Complexes

1. XeF$_2$·2SbF$_5$

XeF$_2$·2SbF$_5$ has been prepared by reaction of SbF$_5$ with either XeF$_2$ or XeF$_4$ (47). It is a yellow, diamagnetic solid which melts at 60°. It sublimes *in vacuo* at 60° and appears to be stable up to at least 120°.

2. XeF$_2$·2TaF$_5$

A complex of composition XeF$_2$·2TaF$_5$ (47) is formed by reaction of TaF$_5$ and XeF$_4$. This complex is straw colored and melts at 81°.

D. Xenon Hexafluoride Complexes (140)

1. XeF$_6$·BF$_3$

Xenon hexafluoride and boron trifluoride combine at room temperature to form the adduct XeF$_6$·BF$_3$. This is a white solid at room temperature melting at 90° to a pale yellow, viscous liquid. The vapor pressure

of the adduct is less than 1 mm. at 20°, although it can be sublimed at this temperature.

Infrared spectra of the vapor indicate that this adduct may be dissociated in the vapor phase.

2. XeF$_6$·AsF$_5$

An adduct of composition XeF$_6$·AsF$_5$ has also been prepared at room temperature. It is considerably less volatile than the BF$_3$ complex at room temperature. The possibility that these complexes may be ionic has been suggested (140).

E. Other Xenon Fluoride Complexes (41)

A compound of approximate composition Xe$_2$SiF$_6$ has been reported. It was prepared by passing mixtures of xenon and fluorine or xenon, fluorine, and SiF$_4$ through an electric discharge in a glass apparatus. The compound is reported to be stable at −78° but decomposes at room temperature.

Another complex, assumed to be XeSbF$_6$, has been prepared by heating mixtures of xenon, fluorine, and SbF$_5$ at 250°. Although the pale yellow product formed was presumed to be different from XeF$_2$·2SbF$_5$ on the basis of its somewhat lower volatility, the evidence for this is not strong.

IV. Other Fluorides and Oxyfluorides

The existence of the three simple binary fluorides and the oxytetrafluoride of xenon has been established beyond doubt. A number of other fluorides and oxyfluorides have been reported. Because these are either unstable or their existence not fully established, they are discussed separately in this section.

A. XeF

The radical XeF has been made by irradiating XeF$_4$ crystals at 77°K. with Co^{60} γ-radiation (49). The irradiated crystal has a blue color which diminishes rapidly in intensity when warmed to 140°K. The electron spin resonance spectrum of the XeF radical (49, 113) has led to the determination of hyperfine interaction constants and g-values for the XeF bond.

A transient species of about 20-μsec. half-life giving rise to bands at 3300 and 2500 Å. has been observed in the flash photolysis of 1:1 Xe/F$_2$ mixtures (175). This species has been tentatively identified as XeF.

B. XeF$_5$

The existence of XeF$_5$ in equilibrium mixtures of Xe and F$_2$ has been reported (176). Subsequent experiments and re-examination of the data (176, 177) have led the authors to withdraw their conclusions as to the existence of this species.

C. XeF$_8$

The synthesis of XeF$_8$ has been reported (151). Xenon–fluorine mixtures in a 1:20 ratio at an initial pressure of 81 atm. were heated to 620° in a nickel

bomb. Continuous pressure measurements during the course of the reaction indicated that a product of average composition $XeF_{6.5}$ was formed. A yellow product, volatile at $-78°$ but trapped at $-195°$, was isolated. It was unstable in glass at room temperature. Analysis of this product for fluorine, obtaining xenon by difference, gave a F/Xe ratio of 8.1 ± 0.1.

These results have not yet been confirmed at other laboratories.

Studies on the xenon–fluorine system (177) indicate that the highest fluoride present in an equilibrium mixture at $250°$ is XeF_6. Moreover, lower temperatures favor the production of higher fluorides.

A plot of the average bond energies (14) against atomic number for the series SbF_5, TeF_6, IF_7 extrapolated to XeF_8 indicates that the average bond energy of XeF_8 may be as high as 24 kcal. This would lead to a standard heat of formation for gaseous XeF_8 of -45 kcal. mole^{-1}. The existence of this molecule can therefore not be ruled out.

D. XeOF₃

The original suggestion that $XeOF_3$ has an independent existence on the basis of mass spectrometric data (160) has been subsequently withdrawn. A product of composition $Xe_{1.2}O_{1.1}F_{3.0}$ allegedly results from the reaction of a 1:1 mixture of xenon and OF_2 in a nickel tube at 300–$400°$ (159). It has been conceded, however, that this product may have consisted of a mixture of fluorides and oxyfluorides.

E. XeO₂F₂

Fragmentation patterns corresponding to XeO_2F_2 have been observed in mass spectrometric analyses of partially hydrolyzed XeF_6 (36). It has not been isolated in weighable quantities (122). The heat of formation of XeO_2F_2 has been calculated from the xenon–oxygen and xenon–fluorine bond energies obtained for XeF_4, XeF_6, and XeO_3. A value of $\Delta H_f°$ of $+35$ kcal. mole^{-1} was obtained, indicating that XeO_2F_2 should be thermally unstable (14).
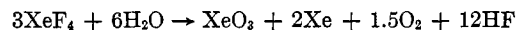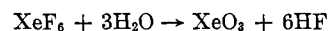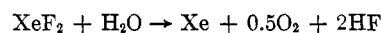
F. XeOF₂

An electric discharge apparatus described previously (159) has been used to cause reaction of 1:1 mixtures of xenon and oxygen difluoride at $195°K$. Transparent crystals in 61% yield were obtained. Although no analytical results were quoted, they allegedly correspond to an empirical formula $XeOF_2$. No properties of this preparation were described, so it is impossible to compare it with another preparation (47) suggested to have the same composition.

The latter was a volatile fraction (b.p. $\sim115°$, m.p. $90°$) obtained as a by-product in the fluorination of xenon at 250–$400°$ by the flow method using oxygen or air as the carrier gas (47).

V. AQUEOUS CHEMISTRY OF XENON

A. GENERAL

Xenon difluoride, tetrafluoride, and hexafluoride react with water as shown in the following reactions (8, 46, 108b, 178). Thus when XeF_6 is hydrolyzed,

$$XeF_2 + H_2O \rightarrow Xe + 0.5O_2 + 2HF$$
$$XeF_6 + 3H_2O \rightarrow XeO_3 + 6HF$$
$$3XeF_4 + 6H_2O \rightarrow XeO_3 + 2Xe + 1.5O_2 + 12HF$$

the xenon is quantitatively retained in solution as hexavalent xenon. When XeF_4 is hydrolyzed, one-third of the xenon is retained in the solution as Xe(VI). The third reaction can be interpreted in terms of the following mechanism.

$$3XeF_4 + 6H_2O \rightarrow 2XeO + XeO_4 + 12HF$$
$$XeO \rightarrow Xe + 0.5O_2$$
$$XeO_4 \rightarrow XeO_3 + 0.5O_2$$

The last reaction is consistent with our knowledge of aqueous Xe(VIII) (8, 108b).

B. PROPERTIES OF AQUEOUS XeF₂ SOLUTIONS (9)

Although rapidly destroyed upon hydrolysis with basic solutions (108b), XeF_2 dissolves unchanged and persists for some time in acid media (half-time at $0°$, 7 hr.). The solutions are colorless and have a pungent odor. The solubility of XeF_2 in water is 25 g./l. at $0°$. The oxidizing species, undissociated XeF_2, is more volatile than water and can be distilled preferentially. It may be extracted into CCl_4, the distribution ratio being about 2.3 in favor of the aqueous phase.

These solutions are powerful oxidants oxidizing HCl to Cl_2, iodate to periodate, Ce(III) to Ce(IV), Co(II) to Co(III), Ag(I) to Ag(II), and alkaline solutions of Xe(VI) to Xe(VIII). The estimated Xe–XeF_2 potential is about 2.2 v. The ultraviolet spectrum of aqueous XeF_2 is very similar to that of gaseous XeF_2 (131).

C. PROPERTIES OF AQUEOUS Xe(VI) ("XENIC ACID")

Pure solutions of Xe(VI) in dilute aqueous acid are colorless, odorless, and stable. The slight decomposition that is sometimes observed is probably due to small amounts of reducing impurities present. Evaporation of these solutions produces solid XeO_3, a powerful explosive. Hexavalent xenon in solution is nonvolatile (8, 178). The reported volatility and instability (91) of Xe(VI) prepared from acid solutions of xenon tetrafluoride can be explained by the presence of XeF_2 impurity (9).

Aqueous solutions as high as 4 M in Xe(VI) have been obtained. Solutions of Xe(VI) are nonconducting (8), indicating that XeO_3 exists in solution as an undissociated species. Additional evidence for this is given

by the Raman spectrum of an aqueous XeO_3 solution (40). This has been interpreted in terms of an un-ionized XeO_3 molecule of symmetry C_{3v}. The Raman frequencies found were 780 (ν_1), 344 (ν_2), 833 (ν_3), and 317 cm.$^{-1}$ (ν_4).

The oxygen exchange between aqueous Xe(VI) and water has been reported to be complete within 3 min. at room temperature (132). Others find the exchange incomplete even after 1 hr. (179). This discrepancy is still unexplained. Conflicting reports on the ultraviolet absorption spectrum of Xe(VI) are also still unresolved (8, 179).

Xe(VI) is reduced at the dropping mercury electrode in a single step to xenon (80). The half-wave potential for this reduction ranges from -0.10 to 0.360 v. against a saturated Hg_2SO_4–Hg reference electrode in the pH range 4.6–8.0.

The Xe(VI)–Xe(0) couple is estimated to be about 1.8 v. in acid and 0.9 v. in base (8). Aqueous xenon(VI) rapidly oxidizes ammonia (presumably to nitrogen), hydrogen peroxide to oxygen, neutral Fe^{2+} to Fe^{3+}, and mercury in 1 N H_2SO_4 to Hg_2SO_4 (179). Chloride is oxidized to chlorine slowly in 2 M HCl and very rapidly in 6 M HCl. Acid manganous solutions are oxidized to MnO_2 over several hours and to permanganate much more slowly (8).

Xenic acid reacts readily with *vic*-diols and primary alcohols in neutral or basic solutions. No reactions are observed in acidic solutions. Analyses of the oxidation products of xenic acid with *vic*-diols yield xenon gas and carboxylic acids or carbon dioxide from the terminal alcohol group (81).

The kinetics of the reactions of Xe(VI) with bromide and iodide have been studied (93). The reactions were observed to obey the following rate laws.
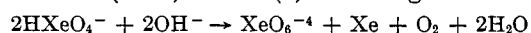
$$\frac{d[Br_2 + Br_3^-]}{dt} = k[XeO_3]_{aq}^{1.19}[H^+]^{2.17}[Br^-]^{2.04}$$

$$\frac{d[I_3^- + I_2]}{dt} = -3\frac{d[XeO_3]_{aq}}{dt} =$$
$$k[XeO_3]_{aq}^{0.94}[I^-]^{0.95}[H^+]^0$$

Only initial slope data were given as there were rapid deviations from linearity, suggesting the possibility of competing reactions. Arrhenius plots of the rate constants give activation energies of 15.5 and 12.2 kcal./mole, respectively. Xe(VI) solutions are very weak acids (46, 178). In strong base the predominant VI species has been postulated to be $HXeO_4^-$ (8), although this species may possibly be hydrated. The equilibrium constant, K_B, for the reaction

$$HXeO_4^- \rightleftarrows XeO_3 + OH^-$$

has been estimated to be $6.7 \pm 0.5 \times 10^{-4}$. The $HXeO_4^-$ species slowly undergoes disproportionation to produce Xe(VIII) and Xe(0) according to

$$2HXeO_4^- + 2OH^- \rightarrow XeO_6^{-4} + Xe + O_2 + 2H_2O$$

A salt of Xe(VI), Ba_3XeO_6, has been reported (91), but this is contradicted by similar preparations (8) which show that although the barium salt immediately precipitated contains Xe(VI), it rapidly disproportionates to give octavalent xenon in the form of Ba_2XeO_6, as well as xenon and oxygen.

D. XENON TRIOXIDE

The hydrolysis of XeF_4 (163, 178) and XeF_6 (154) yields solutions from which colorless crystals of XeO_3 can be obtained by evaporation. This compound is unstable and is a powerful explosive (13, 154, 178). The heat of formation, $\Delta H_f°$, is $+96 \pm 2$ kcal. mole^{-1} (58). The vapor pressure at room temperature is negligible. XeO_3 is hygroscopic (154).

XeO_3 is orthorhombic with unit cell dimensions $a = 6.163 \pm 0.008$, $b = 8.115 \pm 0.010$, $c = 5.234 \pm 0.008$ Å. The probable space group is $P2_12_12_1$. With four molecules per unit cell, the calculated density is 4.55 g. cm.$^{-3}$. The Xe–O bond distances are 1.74, 1.76, and 1.77 Å., each ± 0.03 Å. Bond angles O–Xe–O are 108, 100, and 101°, each $\pm 2°$. The average bond distance, corrected for thermal motion, and the average bond angle are 1.76 Å. and 103°, respectively (163).

Infrared absorption bands have been observed for solid XeO_3. They are: ν_1(A) 770, ν_2(A) 311, ν_3(E) 820, and ν_4(E) 298 cm.$^{-1}$. These were assigned by analogy with ClO_3^-, BrO_3^-, and IO_3^-. The principal stretching force constant is 5.66 mdynes/Å. (152).
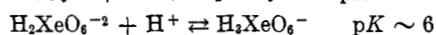
E. PROPERTIES OF AQUEOUS Xe(VIII) (8)

Aqueous Xe(VIII) solutions can be prepared by passing ozone through a dilute solution of Xe(VI) in base. A more practical method is to dissolve sodium perxenate in water according to the reaction

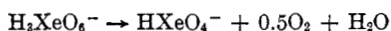$$Na_4XeO_6 + H_2O \rightarrow HXeO_6^{-3} + OH^- + 4Na^+$$

which results in a solution with a pH of about 12.

Perxenate solutions are powerful and rapid oxidizing agents. These solutions oxidize iodide to iodine even in 1 M base, bromide to bromine at pH 9 or less, and chloride to chlorine in dilute acid. Also in dilute acid, Mn^{2+} is immediately converted to MnO_4^-. Rapid oxidation of iodate to periodate and Co(II) to Co(III) occurs in both acid and base solutions. The Xe(VIII)–Xe(VI) couples are estimated to be 0.9 v. in base and 3.0 v. in acid (8).

The ultraviolet absorption spectra of Xe(VIII) are markedly pH dependent. Beer's law is obeyed for 3×10^{-4} to 3×10^{-3} M perxenate over the entire pH range. There are isosbestic points at 220 and 270 mμ, indicating that only two principal species are contributing to the spectra. The ultraviolet spectra in conjunction with potentiometric titrations have been interpreted in terms of the following set of successive protonation reactions.

$$HXeO_6^{-3} + H^+ \rightleftarrows H_2XeO_6^{-2} \quad pK \sim 10.5$$
$$H_2XeO_6^{-2} + H^+ \rightleftarrows H_3XeO_6^{-} \quad pK \sim 6$$

The species $H_3XeO_6^-$ then decomposes liberating oxygen.

$$H_3XeO_6^- \rightarrow HXeO_4^- + 0.5O_2 + H_2O$$

The latter reaction is strongly pH dependent. At pH 11.5 a 0.003 M solution decomposes at a rate of about 1%/hr., while at pH 8 the extent of decomposition exceeds 1%/min. Below pH 7 the decomposition is almost instantaneous.
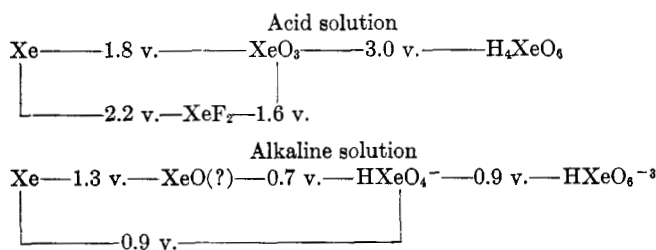
Stable insoluble perxenate salts can be precipitated from Xe(VIII) solutions (8, 108b). In general, sodium perxenate precipitates from solution as $Na_4XeO_6 \cdot 8H_2O$. Upon drying at room temperature, this salt is converted to $Na_4XeO_6 \cdot 2H_2O$. At about 100° the anhydrous salt is formed which is stable to 360° (8). The solubility of sodium perxenate is about 0.025 mole/l. and much less in strong base.

Perxenate salts show an intense infrared band in the 650–680-cm.$^{-1}$ region. This has been identified as the $\nu_3(f_{1u})$ vibration of the octahedral (XeO_6^{-4}) grouping (57).

A mixed valence salt, $K_4XeO_6 \cdot 2XeO_3$, precipitates when Xe(VI) is ozonized in the presence of KOH. The salt is yellow and detonates on drying (8).

F. OXIDATION POTENTIALS

The oxidation potentials of the aqueous xenon species are conveniently summarized below (8, 9).

Acid solution

Xe———1.8 v.————XeO$_3$———3.0 v.———H$_4$XeO$_6$

└——2.2 v.—XeF$_2$—1.6 v.

Alkaline solution

Xe—1.3 v.—XeO(?)—0.7 v.—HXeO$_4^-$—0.9 v.—HXeO$_6^{-3}$

└——0.9 v.——┘

G. PERXENATE SALTS

1. $Na_4XeO_6 \cdot 8H_2O$ (60)

The crystal structure of $Na_4XeO_6 \cdot 8H_2O$ has been determined. The crystals are orthorhombic with cell constants $a = 11.87$, $b = 10.47$, $c = 10.39$ Å. (all ±0.02 Å.). The space group is D_{2h}^{14}-Pbcn. The calculated density is 2.38 g. cm.$^{-3}$. The perxenate ion, XeO_6^{-4}, has approximately the form of a regular octahedron of oxygen atoms surrounding the central xenon atom. The O–Xe–O bond angles do not differ significantly from 90°. The mean bond length is 1.875 Å. with a standard deviation of 0.021 Å.

2. $Na_4XeO_6 \cdot 6H_2O$ (183)

A less common crystalline form, $Na_4XeO_6 \cdot 6H_2O$, occurs when basic Xe(VI) solutions are allowed to disproportionate at 5°. The crystals are orthorhombic,

space group Pbca, with $a = 18.44 \pm 0.01$, $b = 10.103 \pm 0.0007$, and $c = 5.873 \pm 0.005$ Å. The density is calculated as 2.59 g. cm.$^{-3}$ with four molecules per unit cell. The shape of the perxenate ion is the same as that reported for the octahydrate. The average Xe–O distance was found to be 1.84 Å. The O–Xe–O bond angles range from 87.1 to 92.9° with a standard deviation of about 1°. These deviations from 90° were not considered to be significant.

3. $Ba_2XeO_6 \cdot 1.5H_2O$ (8)

Barium perxenate, $Ba_2XeO_6 \cdot 1.5H_2O$, is formed when $Ba(OH)_2$ is added to a Xe(VI) solution. The disproportionation takes place rapidly and is complete within minutes. It is very insoluble in water, a saturated solution in water being only 2.3×10^{-5} M. It decomposes above 300°.

H. XENON TETROXIDE

Gaseous xenon tetroxide was formed by reaction of sodium perxenate with concentrated sulfuric acid. It was identified by mass analysis in a time-of-flight mass spectrometer (70). In general, higher yields are obtained by using barium perxenate, Ba_2XeO_6, rather than the more finely divided sodium salt (139). It is not appreciably volatile at −78°. The vapor pressure at 0° is about 25 mm.

Gaseous xenon tetroxide can be handled at temperatures as high as room temperature, but the compound is unstable and solid samples have exploded at temperatures as low as −40°.
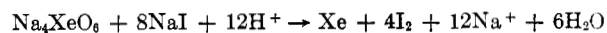
The infrared spectrum of XeO_4 has been obtained. Two bands are definitely assigned to XeO_4. Frequencies for the maxima of the P, Q, and R branches have been given for both bands.

$$\nu_4 \begin{cases} P & 298 \text{ cm.}^{-1} \\ Q & 305.7 \\ R & 314 \end{cases} \qquad \nu_3 \begin{cases} 870 \text{ cm.}^{-1} \\ 877 \\ 885 \end{cases}$$

The data suggest that XeO_4 is a tetrahedral molecule of symmetry T_d. The Xe–O bond length is estimated to be 1.6 ± 0.2 Å. from the P–R separation in the infrared bands.

I. ANALYSIS FOR Xe(VI) AND Xe(VIII) OXIDATION STATES (8)

In acid solution iodide reduces Xe(VI) to elemental Xe (46, 178). The reaction of Xe(VI) with iodide is very slow in base. Xe(VIII) reacts with iodide in both basic and acidic media (8). Acid Xe(VIII) decomposes to give Xe(VI) and O_2. A convenient iodometric method for determination of the valence state of Xe in solution has been worked out (8). Addition of iodide to a solution before acidification gives the total oxidizing power of the solution.

$$Na_4XeO_6 + 8NaI + 12H^+ \rightarrow Xe + 4I_2 + 12Na^+ + 6H_2O$$

Addition of iodide after acidification gives the xenon

$$Na_4XeO_6 + 10H^+ + 6NaI \rightarrow Xe + 0.5O_2 + 3I_2 + \\ 10Na^+ + 5H_2O$$

concentration. The iodine released is determined by titration with thiosulfate.

VI. THE NATURE OF THE CHEMICAL BOND IN THE XENON FLUORIDES

The chemical stability of the xenon compounds seems to violate one of the oldest and most widely accepted rules of valence theory. Indeed, rigid adherence to the octet rule has, until recently, effectively inhibited both theoretical and experimental study of rare gas compounds. Having discovered the existence of stable rare gas compounds without the benefit of theoretical guidance, experimental chemists have, as it were, thrown down the glove and asked for explanation and understanding. Now, a complete *a priori* theoretical study of these molecules would provide binding energies, charge distributions, force constants, etc., in addition to predicting which compounds were stable. At present, an *a priori* analysis of this scope cannot be carried to completion. However, it is possible to make predictions based on semiempirical considerations. The major disadvantage of the semiempirical theory is that unambiguous prediction of the stabilities of different compounds cannot be made. On the other hand, the semiempirical theory does provide a simple and convenient framework with which to correlate a considerable body of experimental data. For example, it is possible to rationalize the geometries of the observed species, to obtain useful estimates of the charge distribution in the ground state, and to interpret the optical spectra of the various compounds, all in terms of an internally consistent scheme.

As might be expected, interpretation of the nature of the chemical bond in rare gas compounds means different things to different people. To date, no *ab initio* calculations of the properties of xenon compounds have been published. Indeed, despite considerable progress in producing Hartree–Fock self-consistent field calculations of molecular structure, the polyatomic xenon compounds are too large to be studied on available computers. Even could such calculations be performed, only the first stage of the calculation would then be complete. The self-consistent field (s.c.f.) wave functions describe an independent electron moving in the average field of all the other electrons in the molecule, and it is conceivable that electron correlation effects not included in the s.c.f. formalism are responsible for a considerable part of the binding energy of the rare gas compounds. The second stage of the calculation, that is, determination of the correlation energy in the molecule, cannot at present be accomplished.

In this review we shall, therefore, consider only *a*

posteriori semiempirical analyses of the molecular structure of the xenon fluorides. Attention is restricted to the xenon fluorides because it is for these compounds that there exists the largest body of experimental data.

Of the several theoretical models proposed to account for the qualitative features of the binding in the xenon fluorides, we elect to discuss first the two extremes, *i.e.*, the electron correlation model and the conventional hybridization model. Following this discussion we turn to the descriptions based on the semiempirical molecular orbital theory and the valence bond theory.

A. THE ELECTRON-CORRELATION MODEL

Molecular structure problems have canonically been treated in either of two approximations: the valence bond scheme or the molecular orbital scheme. A rigorous mathematical framework for the molecular orbital method is provided by the Hartree–Fock–Roothaan equations (133). Each electron is assumed to move, independently, in the average field produced by all the other electrons in the molecule. For a closed-shell system, the ground-state wave function, Ψ_{HFR}, is represented as an antisymmetrized product of molecular orbitals, φ_i, each orbital being itself represented as a linear combination of atomic orbitals, u_p.

$$\Psi_{HFR} = A(\varphi_1(1)\overline{\varphi_1(2)} \ldots \varphi_N(2N-1)\overline{\varphi_N(2N)}) \quad \text{(Eq. 1)}$$

$$\varphi_i = \sum_p C_{pi} u_p \quad \text{(Eq. 2)}$$

This representation naturally leads, *via* the variational principle, to a matrix equation

$$(\mathbf{F} - \varepsilon\mathbf{S})\mathbf{C} = 0 \quad \text{(Eq. 3)}$$

where $\mathbf{F}$, $\mathbf{S}$, and $\mathbf{C}$ are the self-consistent field Hamiltonian matrix, the overlap matrix, and the molecular orbital coefficient matrix, respectively. The energy matrix, ε, is obtained by iterative solution of Eq. 3. Note that the solution of Eq. 3 using the expansion method (134) replaces the direct solution to the Hartree–Fock integro-differential equation. At present this seems the only possible procedure, since direct numerical or analytic solution of the molecular Hartree–Fock equation does not appear feasible. Of course, when carried to completion, the expansion method solution is identical with the direct solution of the Hartree–Fock equation.

The independent electron model does not include the contribution of the instantaneous repulsions between electrons (100, 146). The difference between the exact nonrelativistic total energy and the energy in the Hartree–Fock approximation is called the correlation energy; it is of the order of magnitude of 1–2 e.v. per electron pair.

The restrictions imposed by the Pauli exclusion principle imply that occurrence of collisions between

electrons having parallel spin is unlikely (*i.e.*, every electron is surrounded by a "Fermi hole" (100)). The major error in the independent particle scheme is, therefore, the lack of correlation between electrons with antiparallel spins.

Using these ideas, it has been suggested (2, 4, 109) that the interaction of the xenon atom with ligands of definite spin, say two fluorine atoms, leads to spin-correlated "split" orbitals. Since in this model electrons with α- and β-spins are separated, if a particular ligand has an unpaired electron with spin α, the corresponding xenon orbital occupied by an electron with spin β is attracted toward it, and that orbital occupie dby an electron with spin α is repelled from it. The bonding is then explained as arising from the difference in overlap between the distinct xenon orbitals and the ligand orbital.

The model just described bears a close resemblance to the method of different orbitals for different spins (100), first applied to the He atom where the closed shell $(1s)^2$ is split to form an open shell $(1s'1s'')$. Extension of this method leads to the unrestricted Hartree–Fock scheme (100).

The following difficulties of the correlation model as applied to the xenon fluorides are immediately apparent:

(1) The correlation concept is vaguely defined. It will be assumed that the usual definition (energy and charge distribution changes relative to the restricted Hartree–Fock scheme) is implied.

(2) The distribution of the α- and β-electrons is ill defined. The unrestricted Hartree–Fock scheme does not lead to pure spin states, and the appropriate pure spin component must be selected by means of a projection operator (100). If u and v are the different orbitals for different spins in a two-electron system, the singlet wave function is $\det\{u\alpha, v\beta\} - \det\{v\alpha, u\beta\}$. This function does not provide a clear physical picture of the occupation of the orbitals, since the one-electron charge distribution $\rho(1)$ is

$$\rho(1) = \frac{1}{2}[u^2(1) + v^2(1)] + u(1)v(1)\int u(2)v(2)\,d\tau_2$$

Thus, it appears that one must be extremely careful in making a physical interpretation of the "different orbitals for different spins" method.

(3) The effect of electron correlation on the xenon orbitals is seriously misestimated. The wave function for the one-electron bond is $\det\{A\alpha, B\beta\} - \det\{A\beta, B\alpha\}$, where A and B refer to the two orbitals on the atoms. Once the bond is formed, the concept of attraction and repulsion between the xenon and the ligand orbitals with antiparallel and parallel spins, respectively, is meaningless.

(4) The model is not specific. The correlation energy upon molecule formation seems to be independent of the

size of the atom (6). This model does not explain why other xenon compounds (say XeI_4) are unstable.

Let the exact wave function of the system be written in the form (146)

$$\Psi = \Psi_{HFR} + \chi \qquad (Eq.\ 4)$$

where the function χ, representing the correlations not included in the Hartree–Fock scheme, is given by (146)

$$\langle \chi | \Psi_{HFR} \rangle = 0 \qquad (Eq.\ 5)$$

$$\chi = \sum_{i=1}^{N} \{\hat{f}_i\} + \sum_{i>j}^{N} \{\hat{U}_{ij}'\} + \sum_{i>j>k}^{N} \{\hat{U}_{ijk}'\} + \ldots$$

$$(Eq.\ 6)$$

with the successive terms representing one, two, three, … electron excitations.

The application of Brillouin's theorem (24) to the interaction between Hartree–Fock configurations shows that the effect of one-electron excitations is small. The major contribution to the correlation energy arises from electron pair correlations and composite pair-pair correlations.

In view of the small contribution of one-electron excitations to χ, it is expected that the Hartree–Fock approximation, which includes the effects of long-range interelectronic repulsions adequately, will lead to an accurate ground-state charge distribution (146). Since a major part of the effect of the distortion of atomic orbitals upon molecule formation is included in the s.c.f. approximation, it is also expected that core polarization effects (*i.e.*, core-valence electron correlation energy changes) will be very small, possibly not exceeding 0.1 e.v. (146).

Recent studies have shown that the F_2 molecule is unbound in the Hartree–Fock–Roothaan scheme (168). Nevertheless, except for the binding energy, the other ground-state properties (intermolecular distance, force constant) are properly accounted for (168). This extreme example demonstrates the important contribution of correlation effects to the binding energy and their minor effect on the charge distribution. It is expected that a similar situation will arise in the case of the xenon fluorides. The correlation energy change upon the formation of the molecule XeF_n is defined as

$$\Delta E^{corr} = E^{cor}(XeF_n) - E^{cor}(Xe) - nE^{cor}(F)$$

$$(Eq.\ 7)$$

Since one $5p^2$ electron pair in the xenon atom is decoupled on the formation of two Xe–F bonds, it is expected that the contribution of correlation energy will be of the order of 0.5 to 1 e.v. per bond. Thus, correlation effects (which are a mathematical rather than a physical concept) do not provide any new description of the binding in the xenon fluorides.

B. THE HYBRIDIZATION MODEL

A conventional bonding scheme, involving pd or ps hybrids, may be provided for the xenon fluorides (5, 76, 88) and for the xenon–oxygen compounds (54, 61, 169, 181, 182). Consider first the molecule XeF_4. The description of electron-pair bonds is preserved if sp^3d^2 hybrids constructed from atomic orbitals are used (5, 76). The xenon atom is expected to provide eight valence electrons and each of the four fluorine atoms to provide one electron, so that six electron pairs are formed. There then result four coplanar bonds and two lone pairs of electrons. In a similar manner, the linear structure of XeF_2 can be interpreted in terms of linear sp hybrids.

The hydridization model may be criticized on the basis of the following two considerations:

(a) The excitation energies $5s^25p^6 \rightarrow 5s^25p^55d$ and $5s^25p^6 \rightarrow 5s^25p^56s$ in the xenon atom are of the order of magnitude of 10 e.v. (112), while the gain in energy by molecule formation cannot be large enough to compensate for the promotion energy to the valence state. Formation of a stable compound under such conditions is unlikely. A semiempirical estimate of $np \rightarrow nd$ promotion energies in the rare gas atoms has been made (64) using the experimental polarizabilities and the diamagnetic susceptibilities. The effective promotion energy was expressed in the form (64)

$$\Delta E_{np \rightarrow nd} = \frac{8}{3} \frac{e^2 \langle r_i{}^2 \rangle}{\alpha(np \rightarrow nd)} \qquad \text{(Eq. 8)}$$

where $\langle r_i{}^2 \rangle$ is the mean-square radius of the np orbital and $\alpha(np \rightarrow nd)$, the contribution of the $np \rightarrow nd$ excitation to the atomic polarizability; this latter value was estimated to be 75% of the total polarizability. The $5p \rightarrow 5d$ promotion energy for the xenon atom was then found to be 16.6 e.v., so that the effect of d-hybridization is expected to be small.

(b) The existence of XeF_6 would require fourteen valence electrons (in an sp^3d^2 scheme (5)), and this cannot be accommodated within the considerations given above. The existence of XeF_6 therefore appears to rule out this model independently of energy difficulties. An octahedral XeF_6 could be formed (43) by using $p_z \pm d_{z^2}$, $p_x \pm d_{x^2}$, and $p_y \pm d_{y^2}$ orbitals, but these six orbitals are not orthogonal, and the scheme requires an impossibly large amount of energy for the several $p \rightarrow d$ promotions in the valence-state preparation.

It is possible to view the hybridization model as a localized bond scheme. Any ground-state, closed-shell, polyatomic molecule can be described in terms of equivalent localized orbitals involving electron pairs. This follows directly from the properties of the determinental wave function, which is invariant under unitary transformations (129, 133). While the equiv-

alent orbitals description still maintains the conventional electron-pair bond, the charge distribution (*i.e.*, ionic character) within the bond is determined by the coefficients of the constituent molecular orbitals. Having removed even the necessity of describing localized bonds by hybrid orbitals, we believe that the hybridization model is inadequate to describe bonding in the xenon fluorides. Of course, some hybridization is required, *e.g.*, in the form of orbital polarization.

C. LONG-RANGE XENON–FLUORINE INTERACTIONS

Semiempirical theoretical studies of molecular structure suffer from the disadvantage that unambiguous predictions of molecular stability are not possible. In view of this observation, some criterion of applicability must be adopted before the predictions of any simple one-electron model description can be accepted (86). Now, much of the work on the xenon fluorides has been done within the framework of the simplest delocalized molecular orbital scheme. The use of delocalized bonding orbitals must be viewed with caution, since the naïve delocalized molecular–orbital scheme leads to a stabilization of H_3 relative to H_2 and H (166). In the H_2 + H system, intermolecular dispersion forces are weak, and repulsive forces keep the H and H_2 apart. In order for the delocalization model to be applicable and lead to binding, it is necessary that long-range attractive forces be operative (86).

Therefore, to validate the use of delocalized molecular orbitals and to account for the binding in the xenon fluorides, long-range interactions between xenon and fluorine atoms must be considered. It is well known that the molecular orbital description breaks down for distances larger than about one and one-half times the equilibrium internuclear separation, and that the valence-bond description must be used in this range (44). The weak long-range interactions we wish to discuss can be adequately described in terms of the Mulliken charge-transfer theory (116, 117). Consider the XeF diatomic molecule at large Xe–F separation ($R > 3$ Å.). In this system the xenon atom acts as an electron donor, while the fluorine atom acts as an electron acceptor. Using a semiempirical valence-bond scheme (86), it has been shown that charge-transfer interactions are quite strong because of the relatively large overlap between the filled $5p\sigma$ orbital of xenon and the vacant $2p\sigma$ fluorine atom orbital. The long-range stabilization of the Xe–F pair is assigned to σ-type interaction with the system described in terms of resonance between the "no bond structure" (which may of course be stabilized by dispersion forces) and the ionic dative structure, Xe^+F^-. The valence bond wave function is

$$\Psi = \Psi_0(XeF) + \alpha\Psi_1(Xe^+F^-) \qquad \text{(Eq. 9)}$$

where α is a mixing coefficient. The charge-transfer

stabilization energy is given by the second-order perturbation theory expression

$$\Delta E^{CT} = -\frac{(H_{01} - S_{01}H_{00})^2}{H_{00} - H_{11}} \qquad \text{(Eq. 10)}$$

where the H_{ij} values are the matrix elements of the total Hamiltonian for the system, and S_{01} is the overlap integral between the states Ψ_0 and Ψ_1. Application of a one-electron treatment and approximation of the exchange integrals using the Mulliken magic formula lead to the result

$$\Delta E^{CT} = -\frac{2S^2}{1 + S^2} \frac{\left(A_F + \dfrac{e^2}{2R}\right)^2}{\left(I_{Xe} - A_F - \dfrac{e^2}{R}\right)} \qquad \text{(Eq. 11)}$$
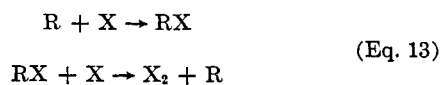
where A_F is the electron affinity of a fluorine atom ($A_F = 3.45$ e.v.), I_{Xe} is the ionization potential of xenon (12.1 e.v.), and R is the Xe–F separation. S is the overlap integral between the filled Xe $5p\sigma$ and the empty F $2p\sigma$ orbitals.

In addition to the charge-transfer interaction, there is a sizable contribution to the binding energy from the (second-order) dispersion forces ΔE^{dis}. These can be represented in the conventional form (86)

$$\Delta E^{dis} = -\frac{3}{2} \frac{I_{Xe}I_F}{I_{Xe} + I_F} \frac{\alpha_{Xe}\alpha_F}{R^6} \qquad \text{(Eq. 12)}$$

Using the known polarizabilities and ionization energies, it is easily shown that, in the case of Xe + F, dispersion and charge-transfer interactions are dominant at large internuclear separation. Indeed, the charge-transfer interaction is larger than the dispersion interaction by an order of magnitude, and both are attractive interactions (86). This simplified treatment of charge transfer and dispersion forces (which include higher-order effects not contained within the s.c.f. scheme) is a semiempirical one-electron scheme based on experimental data.

It is seen that charge-transfer interactions lead to binding energies of the order of magnitude of a few kilocalories per mole and cannot alone account for molecule formation (116, 117). Nevertheless, there is some evidence from studies of halogen atom recombination, as catalyzed by inert gases, that these interactions are important. It is fairly well established (130) that the recombination of halogen atoms involves a diatomic radical formed from a halogen atom, X, and an inert gas atom, R

$$R + X \rightarrow RX$$

$$RX + X \rightarrow X_2 + R \qquad \text{(Eq. 13)}$$

Studies of the *negative* energies of activation of these reactions (130) indicate that the heat of formation of the complex RX is greater than can be accounted for using dispersion interactions only. The estimated HeI and ArI interaction energies are 1 and 2 kcal./mole, respectively. Charge-transfer interactions have been invoked to account for the surplus binding energy (130).

In the case of the Xe + F interaction, the pattern of charge transfer is quite well defined: the rare gas atom acts as the electron donor and the F atom as the electron acceptor. For pairwise interactions involving other rare gas atoms, characterized by higher ionization potentials (I), the situation is not so well defined. For example, in HeI it is expected that the iodine atom ($I = 10.4$ e.v.) will act as the electron donor, while the helium atom ($I = 25$ e.v.) will act as the electron acceptor. In spite of the negative (unknown) electron affinity of the helium atom, the ionic configuration I^+He^- is expected to be stabilized relative to the neutral configuration HeI by electrostatic interactions, and thereby to contribute to the over-all stabilization of the collision complex. In those cases when the ionization potential of the rare gas atom is of the same order of magnitude as that of the halogen atom, two-way charge-transfer stabilization (117) is expected to occur.

Spectroscopic evidence for weak charge-transfer interactions involving rare gas atoms has recently been obtained from the study of the ultraviolet spectrum of nitric oxide in a krypton matrix at 4°K. (128). This system reveals an intense absorption band with an onset at 2500 Å. which cannot be assigned to the NO γ-system (128). A plausible interpretation (52) of this absorption band involves an excited state of the configurational form Kr^-NO^+, where the NO molecule ($I_{NO} = 9.9$ e.v.) acts as the electron donor, while the Kr atom ($I_{Kr} = 14$ e.v.) acts as the electron acceptor. Since the charge-transfer absorption band almost overlaps the NO absorption band, there is expected to be considerable mixing of the ionic and neutral states. Theoretical evidence is also available for an important contribution of charge-transfer states to the first exciton band of pure rare gas solids (173).

The results of the theoretical treatment of the charge-transfer interactions between xenon and fluorine atoms provide a necessary (but by no means sufficient) criterion for the applicability of the one-electron molecular orbital scheme. Lowering the energy of the system by charge-transfer interactions indicates that the ground state constructed in the molecular orbital approximation will lead to a reasonable approximation for the ground state of the bound system. At smaller Xe–F separations, the second-order perturbation theory used breaks down, and molecular orbital theory or valence bond theory based on the variation method must be employed, although similar trial wave functions may be used.

D. THE MOLECULAR ORBITAL MODEL

The molecular orbital (MO) model used to describe the xenon fluorides follows conventional lines (4, 21, 23, 64, 77, 83, 86, 96, 98, 99, 125, 127, 135). The bonding in compounds of xenon and fluorine has been described in terms of delocalized molecular orbitals formed mainly by combination of $p\sigma$-type xenon and fluorine orbitals (83, 86, 135). Thus, in XeF_2, one doubly filled Xe $5p\sigma$ atomic orbital and two F $2p\sigma$ atomic orbitals, each containing one electron, are considered. Similar considerations apply to XeF_4, starting with four F $2p\sigma$ and two Xe $5p\sigma$ orbitals. In a zeroth approximation, xenon and fluorine $np\pi$ and ns orbitals, and xenon d-type orbitals can be considered to be nonbonding. More elaborate calculations have included the effects of π-bonding (86, 98, 99) and introduced Xe $5s$, $4d$, and $5p$ and fluorine $2s$ orbitals into the MO scheme (21, 22, 98, 99).

The semiempirical treatment is reduced to a simple LCAO theory equivalent to the treatment of heteroatomic, π-electron systems (45), except for the different symmetries of the orbitals involved. In the standard LCAO scheme the molecular orbitals, φ_r, are represented in the form

$$\varphi_r = \sum_i C_{ri}u_i \qquad \text{(Eq. 14)}$$

where the u_i's are atomic orbitals. The secular equations are

$$[\alpha(i) - E_i]C_{ri} + \sum_{j \neq i} [\beta(i, j) - E_r S(ij)]C_{rj} = 0 \qquad \text{(Eq. 15)}$$

The matrix elements may be written in terms of the effective one-electron Hamiltonian, h (not very clearly defined in this scheme), so that the Coulomb integral is given by

$$\alpha(i) = \langle u_i|h|u_i \rangle \qquad \text{(Eq. 16)}$$

the exchange integral is

$$\beta(i,j) = \langle u_i|h|u_j \rangle \qquad \text{(Eq. 17)}$$

and the overlap integral is given by

$$S(i,j) = \langle u_i|u_j \rangle \qquad \text{(Eq. 18)}$$

The total orbital energy is then

$$\epsilon = \sum_r m_r E_r \qquad \text{(Eq. 19)}$$

where m_r is the occupation number of the rth molecular orbital. The energy of the atoms at infinite separation is taken as

$$I_\epsilon = \sum_i m_i\alpha(i) \qquad \text{(Eq. 20)}$$

with m_i being the occupation number of the ith atomic orbital in the atoms in their ground states. The binding energy per bond (considering N bonds in the molecular system) is then approximated by (86, 98, 99)

$$\Delta E = \frac{I_\epsilon - \epsilon}{N} \qquad \text{(Eq. 21)}$$

The approximations involved in the derivation of Eq. 21 must now be considered (86, 99). The sum of the orbital energies is not equal to the total energy of an atomic or molecular system in the Hartree–Fock self-consistent field scheme, because all Coulomb repulsions between electron pairs and exchange interactions between electrons with parallel spins have not been properly included. To the extent that the one-electron effective Hamiltonian, h, represents a s.c.f. Hamiltonian, Eq. 19 includes the interelectronic Coulomb repulsion energy, $\sum_{r>s} J_{rs}$, twice. On the other hand, the internuclear repulsion term, V_{nn}, has been omitted from the molecular energy expression. When these effects are taken into account (and when exchange effects are neglected), Eq. 21 becomes

$$\Delta E = \frac{1}{N}\left(I_\epsilon - \epsilon + \sum_{r>s} J_{rs} - V_{nn}\right) \qquad \text{(Eq. 22)}$$

In the derivation of Eq. 21, it is assumed that the last two terms in Eq. 22 cancel (65, 148). However, this cancellation is by no means exact even for simple molecular systems (148), and the absolute values of binding energies derived from Eq. 21 are usually overestimates by a factor of 2–3. The semiempirical LCAO method cannot be expected to lead to reliable values of bond energies, which are not easily obtained even by much more elaborate SCF computations. On the other hand, the semiempirical treatment is expected to be extremely useful for the computation of energy differences between nuclear or electronic configurations.

The eigenvectors of the secular matrix yield information concerning the charge distribution in the molecule. This calculation is to be carried out taking account of the nonorthogonality of the atomic orbitals. The normalization condition for φ_r is given by (42)

$$\sum_{i,j} S(i,j)C_{ri}C_{rj} = 1$$

and the overlap integrals may be regarded as the components of the metric tensor in the space defined by the MO coefficients. Consider the set

$$d_{ri} = \sum_j S(i,j)C_{rj} \qquad \text{(Eq. 23)}$$

Then the charge on atom i, q_i, can be expressed in the form

$$q_i = \sum_r m_r C_{ri}d_{ri} \qquad \text{(Eq. 24)}$$

Before proceeding, let us examine some qualitative features of the bonding as described by the molecular

TABLE VI

SYMMETRY ORBITALS FOR LINEAR XeF₂, SQUARE-PLANAR XeF₄, AND OCTAHEDRAL XeF₆

	Symmetry group	Orbital symmetry	Xenon orbital	Fluorine orbitals	
				σ	π
XeF₂	$D_{\infty h}$	a_{1g}	s, d_{z^2}	$\sigma_1 - \sigma_2$	
		a_{2u}	p_z	$\sigma_1 + \sigma_2$	
		e_{1u}	$\begin{cases} p\pi_x \\ p\pi_y \end{cases}$		$p\pi 1_x + p\pi 2_x$ $p\pi 1_y + p\pi 2_y$
		e_{1g}	$\begin{cases} d_{zx} \\ d_{zy} \end{cases}$		$p\pi 1_x - p\pi 2_x$ $p\pi 1_y - p\pi 2_y$
		e_{2g}	$\begin{cases} d_{x^2-y^2} \\ d_{zy} \end{cases}$		
XeF₄	D_{4h}	a_{1g}	s, d_{z^2}	$\sigma_1 + \sigma_2 + \sigma_3 + \sigma_4$	
		e_u	$\begin{cases} p_x \\ p_y \end{cases}$	$\sigma_1 - \sigma_3$ $\sigma_2 - \sigma_4$	$p\pi 2_y - p\pi 4_x$ $p\pi 1_x - p\pi 3_y$
		a_{2u}	$p\pi_z$		$p\pi 1_y + p\pi 2_x - p\pi 2_x\ p\pi 4_y$
		b_{1g}	$d_{x^2-y^2}$	$\sigma_1 - \sigma_2 + \sigma_3 - \sigma_4$	
		b_{2g}	d_{xy}		$p\pi 1_x + p\pi 2_y + p\pi 3_y + p\pi 4_x$
		e_g	$\begin{cases} d_{zx} \\ d_{zy} \end{cases}$		$p\pi 1_y + p\pi 3_x$ $p\pi 2_x + p\pi 4_y$
		b_{2u}			$p\pi 2_x - p\pi 1_y + p\pi 3_x - p\pi 4_y$
		a_{2g}			$p\pi 1_x - p\pi 2_y - p\pi 4_x + p\pi 2_x$
XeF₆	O_h	a_{1g}	s	$\sigma_1 + \sigma_2 + \sigma_3 + \sigma_4 + \sigma_5 + \sigma_6$	
		e_g	$d_{x^2-y^2}$	$\sigma_1 - \sigma_2 + \sigma_4 - \sigma_5$	
			d_{z^2}	$2\sigma_3 + 2\sigma_6 - \sigma_1 - \sigma_2 - \sigma_4 - \sigma_5$	
		t_{1u}	p_x	$\sigma_1 - \sigma_4$	$p\pi 3_x + p\pi 2_y - p\pi 5_x - p\pi 6_y$
			p_y	$\sigma_2 - \sigma_5$	$p\pi 1_x + p\pi 3_y - p\pi 6_x - p\pi 4_y$
			p_z	$\sigma_3 - \sigma_6$	$p\pi 2_x + p\pi 1_y - p\pi 4_x - p\pi 5_y$
			d_{zx}		$p\pi 3_x + p\pi 1_y + p\pi 4_x + p\pi 6_y$
		t_{2g}	d_{yz}		$p\pi 2_x + p\pi 3_y + p\pi 6_x + p\pi 5_y$
			d_{xy}		$p\pi 1_x + p\pi 2_y + p\pi 5_x + p\pi 4_y$

orbital scheme. Consider the molecule XeF₂. If the three atoms are collinear, it is easy to see that the 2p orbitals of the F atoms and the 5p orbitals of the Xe atom can be arranged so that there is extensive overlap. Moreover, the inner portion of the Xe 5p orbital, which has several nodes, contributes very little to the total overlap. Since most of the overlap occurs in the region midway between the nuclei (when at the equilibrium internuclear spacing), it is easy to see that on account of greater overlap, the largest binding energy for XeF₂ will occur for a linear geometry (43). Similar arguments when applied to XeF₄ lead to the expectation that the molecule is planar and of symmetry D_{4h} (43).

We now return to a study of the details of the semi-empirical treatment of xenon fluorides. In Table VI we have listed the symmetry orbitals proper to XeF₂, XeF₄, and XeF₆, constructed by standard group theoretical methods. The phase convention follows previous work (10, 86). The effect of Xe 5s, 6s, 4d, and 5d and the fluorine 2s and 3s orbitals will be neglected. By linear combination of three atomic orbitals, three molecular orbitals of σ-symmetry may be constructed. The three appropriate σ-type molecular orbitals for linear XeF₂ are represented by

$$\varphi(a_{2u}^-) = \frac{a_-}{\sqrt{2}}(\text{F } p\sigma 1 - \text{F } p\sigma 2) + b_-(\text{Xe } p\sigma)$$

$$\varphi(a_{1g}) = \frac{1}{\sqrt{2}}(\text{F } p\sigma 1 + \text{F } p\sigma 2) \qquad \text{(Eq. 25)}$$

$$\varphi(a_{2u}^+) = \frac{a_+}{\sqrt{2}}(\text{F } p\sigma 1 - \text{F } p\sigma 2) + b_+(\text{Xe } p\sigma)$$

while the π-type orbitals are represented by

$$\varphi(e_{1u}) = \beta\binom{\text{Xe } p\pi_x}{\text{Xe } p\pi_y} + \alpha\binom{\text{F } p\pi 1_x + \text{F } p\pi 2_x}{\text{F } p\pi 1_y + \text{F } p\pi 2_y}$$

$$\text{(Eq. 26a)}$$

and

$$\varphi(e_{1g}) = \frac{1}{\sqrt{2}}\binom{\text{F } p\pi 1_x - \text{F } p\pi 2_x}{\text{F } p\pi 1_y - \text{F } p\pi 2_y} \qquad \text{(Eq. 26b)}$$

The secular determinant is readily factorized, leading to the energy levels (4, 83, 86)

$$E_{\pm}(a_{2u}) = \frac{A \pm \sqrt{(A^2 - B)}}{2C} \qquad \text{(Eq. 27)}$$

where

$$A = \alpha(\text{Xe}) + \alpha(\text{F}) -$$
$$4\beta(\text{Xe } p\sigma, \text{ F } p\sigma)S(\text{Xe } p\sigma, \text{ F } p\sigma) \quad \text{(Eq. 28)}$$

$$B = 4C[\alpha(\text{Xe})\alpha(\text{F}) - 2\beta^2(\text{Xe } p\sigma, \text{ F } p\sigma)] \qquad \text{(Eq. 29)}$$

and

$$C = 1 - 2S^2(\text{Xe } p\sigma, \text{ F } p\sigma) \qquad \text{(Eq. 30)}$$

$$E(a_{1g}) = \alpha(F) \qquad \text{(Eq. 31)}$$

Since the σ-orbitals are responsible for bonding in these compounds, they will be considered first.

The energies of the σ-type orbitals are in the sequence $E(a_{2u}{}^-) < E(a_{1g}) < E(a_{2u}{}^+)$ so that in the ground state of XeF$_2$ the bonding $\varphi(a_{2u}{}^-)$ and the nonbonding φ-(a_{1g}) orbitals are doubly occupied while the antibonding $\varphi(a_{2u}{}^+)$ orbital is empty.

The energy levels for the π-type orbitals are of similar form. The two orbital energies $E_{\pm}(e_{1u})$ are obtained from Eq. 27 by substituting $\beta(\text{Xe }\pi, \text{ F }\pi)$ and $S(\text{Xe }\pi, \text{ F }\pi)$ for $\beta(\text{Xe }\sigma, \text{ F }\sigma)$ and $S(\text{Xe }\sigma, \text{ F }\sigma)$, respectively. Three doubly degenerate occupied π-orbitals $e_{1u}{}^-$, e_{1g}, and $e_{1u}{}^+$ are thus formed. Now, the orbitals a_{1g} and e_{1g} are very close in energy to the fluorine 2p atomic orbitals, because overlap in these cases is very small. In a higher approximation in which the xenon 5dσ and 5dπ orbitals are included, both the a_{1g} and e_{1g} orbitals will be depressed in energy, with the a_{1g} orbital probably lying lower than the e_{1g} orbital because σ-overlap is usually larger than π-overlap. Also, because of the larger overlap, the spread of the energies of the σ-orbitals will exceed the spread of the energies of π-orbitals. It is thus concluded that in the absence of spin-orbit coupling the order of orbital energies will be $5s < a_{2u}{}^- < e_{1u}{}^- < a_{1g} \lesssim e_{1g} < e_{1u}{}^+ < a_{2u}{}^+ < 5d$. The ground state configuration of XeF$_2$ becomes, then,

$$(a_{2u}{}^-)^2(e_{1u}{}^-)^4(a_{1g})^2(e_{1g})^4(e_{1u}{}^+)^4 \quad (43)$$

or

$$(a_{2u}{}^-)^2(e_{1u}{}^-)^4(e_{1g})^4(a_{1g})^2(e_{1u}{}^+)^4 \quad (86)$$

Since in the ground state of XeF$_2$ the π-orbitals are completely filled, the π-electron distribution is the same as if the electrons remained on their separated nuclei, confirming that the bonding is of σ-type. In particularly perceptive terms, the σ-orbitals $(a_{2u}{}^-)^2$ $(a_{1g})^2$ have been described as forming a three-center four-electron bond (135) thereby emphasizing the nature of the delocalization, the charge transfer, and the closed-shell character. In this respect, an alternative representation of the ground state wave function of XeF$_2$ is of some interest. It can be easily shown that the ground state wave function, for this system, described by a single Slater determinant reduces to a form characteristic of two localized Xe–F bonds. We may, for the sake of this argument, consider only orbitals with one spin function. Since the determinantal function is invariant under a unitary transformation (129), it is apparent that (86)

Thus, the term "delocalization" should not be interpreted in a literal sense. The transformed orbitals represent localized Xe–F bonds, but these new orbitals are not orthogonal and are not useful for making estimates of the charge distribution. Such localized orbitals have been used (171) as a basis for the description of bonds in the rare gas halides, but this treatment is open to criticism because of the nonorthogonality of the orbitals.

The simple MO treatment involving pσ orbitals leads to some interesting conclusions, independent of the numerical values assigned to the molecular integrals (43, 86). Consider a comparison of the bond energies of XeF$_2$ and the radical XeF. The bond energy per Xe–F bond in linear XeF$_2$ is $\alpha(\text{Xe}) - E_-$. Now, the XeF diatomic radical can be treated as a two-center three-electron problem. The secular equation leads to the two energy levels E_+ and E_- represented by Eq. 27, with the level E_- doubly occupied and E_+ singly occupied. The σ-orbital energy of the $^2\Sigma$ XeF ground state is thus $2E_- + E_+$, while the bond energy is

$$2\alpha(\text{Xe}) + \alpha(\text{F}) - (2E_- + E_+) =$$
$$[\alpha(\text{Xe}) + \alpha(\text{F}) - (E_+ + E_-)] +$$
$$[\alpha(\text{Xe}) - E_-] \quad \text{(Eq. 33)}$$

Because of the nonorthogonality correction (note that β is negative) in Eq. 27, $\alpha(\text{Xe}) + \alpha(\text{F}) - (E_+ + E_-) < 0$; hence, the bond energy in the XeF radical is expected to be less than the bond energy (per bond) in XeF$_2$.

At this point it is convenient to examine the hypothetical bent structure (bond angle 90°) of XeF$_2$ (43, 86, 98). In this problem there are six electrons located in four σ-type molecular orbitals (two Xe pσ and two F orbitals). The four energy levels are E_- and E_+, each doubly degenerate. The ground state of this molecule is, therefore, a triplet state, and the bond energy is

$${}^{1}/_{2}[4\alpha(\text{Xe}) + 2\alpha(\text{F}) - 4E_- - 2E_+] \quad \text{(Eq. 34)}$$

But this is just the bond energy of the XeF radical (Eq. 33). Hence, we may conclude that the bent structure (bond angle 90°) of XeF$_2$ is less stable than the corresponding linear structure.

Consider now the structure of the square-planar XeF$_4$ molecule (symmetry group D$_{4h}$). The molecular orbitals can be readily constructed from the symmetry

$$\begin{vmatrix} \varphi(a_{2u}{}^-)(1) & \varphi(a_{2u}{}^-)(2) \\[2ex] \varphi(a_{1g})(1) & \varphi(a_{1g})(2) \end{vmatrix} = \begin{vmatrix} \left[\sqrt{a_-}(\text{F p}\sigma 1) + \dfrac{b_-}{a_-\sqrt{2}}(\text{Xe p}\sigma) \right](1) & \left[\sqrt{a_-}(\text{F p}\sigma 1) + \dfrac{b_-}{a_-\sqrt{2}}(\text{Xe p}\sigma) \right](2) \\[3ex] \left[\sqrt{a_-}(\text{F p}\sigma 2) - \dfrac{b_-}{a_-\sqrt{2}}(\text{Xe p}\sigma) \right](1) & \left[\sqrt{a_-}(\text{F p}\sigma 2) - \dfrac{b_-}{a_-\sqrt{2}}(\text{Xe p}\sigma) \right](2) \end{vmatrix}$$

$$\text{(Eq. 32)}$$

orbitals presented in Table VI. It should be noted that the doubly degenerate e_u σ-type orbital involves a contribution from the fluorine π-type orbitals. This molecular orbital is given in the form

$$\varphi(e_u) = \begin{cases} A(\text{Xe } p\sigma_x) + \dfrac{a}{\sqrt{2}}(\text{F } p\sigma1_z - \text{F } p\sigma3_z) + \\[2mm] \qquad \dfrac{b}{\sqrt{2}}(\text{F } p\pi2_y - \text{F } p\pi4_x) \\[4mm] A(\text{Xe } p\sigma_y) + \dfrac{a}{\sqrt{2}}(\text{F } p\sigma2_z - \text{F } p\sigma4_z) + \\[2mm] \qquad \dfrac{b}{\sqrt{2}}(\text{F } p\pi1_y - \text{F } p\pi3_y) \end{cases}$$

(Eq. 35)

where A, a, and b are the MO coefficients. The three e_u-type energy levels (*i.e.*, two doubly degenerate σ-levels and one doubly degenerate π-level) were obtained neglecting the interaction between pairs of fluorine atoms separated by 3.9 Å.

The other σ-type orbitals in XeF_4 can be represented in the form

$$\varphi(b_{1g}) = \frac{(\text{F } p\sigma1_z) - (\text{F } p\sigma2_z) + (\text{F } p\sigma3_z) - (\text{F } p\sigma4_z)}{2[1 - 2S(\text{F } p\sigma1_z, \text{F } p\sigma2_z)]^{1/2}}$$

$$\varphi(a_{1g}) = \frac{(\text{F } p\sigma1_z) + (\text{F } p\sigma2_z) + (\text{F } p\sigma3_z) + (\text{F } p\sigma4_z)}{2[1 + 2S(\text{F } p\sigma1_z, \text{F } p\sigma2_z)]^{1/2}}$$

(Eq. 36a)

It should be noted that the interaction between adjacent fluorine atoms (separated by 2.82 Å.) cannot now be neglected. The corresponding orbital energies are

$$E(b_{1g}) = \frac{\alpha(\text{F}) - 2\beta(\text{F } p\sigma1_z, \text{F } p\sigma2_z)}{1 - 2S(\text{F } p\sigma1_z, \text{F } p\sigma2_z)}$$

$$E(a_{1g}) = \frac{\alpha(\text{F}) + 2\beta(\text{F } p\sigma1_z, \text{F } p\sigma2_z)}{1 - 2S(\text{F } p\sigma1_z, \text{F } p\sigma2_z)}$$

(Eq. 36b)

Thus the interaction between adjacent F $p\sigma$ orbitals which are perpendicular to each other leads to a splitting of the orbital energies. The energy difference is given by

$$E(b_{1g}) - E(a_{1g}) =$$

$$\frac{2\alpha(\text{F})S(\text{F } p\sigma1_z, \text{F } p\sigma2_z) - 4\beta(\text{F } p\sigma1_z, \text{F } p\sigma2_z)}{1 - 4S^2(\text{F } p\sigma1_z, \text{F } p\sigma2_z)}$$

(Eq. 36c)

In the ground state of XeF_4, the $e_u{}^+$ orbital is empty, and the state of the molecule is $^1A_{1g}$.

Detailed numerical calculations, based on the preceding analysis, have been performed (21, 22, 64, 86, 96, 98, 99). It should be borne in mind that the numerical results obtained from a semiempirical scheme are quite sensitive to the approximations used. Slater-type atomic orbitals were used for the Xe and F atoms to account for the interactions at separations of the order of the equilibrium interatomic distances. The orbital exponents were obtained either from Slater rules or by fitting to experimental atomic diamagnetic susceptibility data. For the interaction between adjacent F atoms in XeF_4, the use of Slater-type orbitals is inappropriate because of the large distances involved (2.8 Å.); therefore, self-consistent field F-atom wave functions were used. The Coulomb integrals were taken as the atomic ionization potentials or valence state ionization potentials (Table VII), and the exchange integrals were taken to be proportional to the overlap integrals

$$\beta(i,j) = K(i,j)S(i,j) \qquad \text{(Eq. 17a)}$$

TABLE VII

COULOMB INTEGRALS FOR SEMIEMPIRICAL MO CALCULATIONS FOR THE XENON FLUORIDES

Orbital	Coulomb integrals, e.v.		
	a	b	c
Xe 6s	−2.5	...	−3.2
Xe 5d	−2.0	...	−2.0
Xe 5p	−12.1	−15.0	−12.3 (σ), −11.3 (π)
Xe 5s	−23.0	−30.0	−27.0
Xe 4d	−25.0	−25.0	...
F 2p	−17.4	−17.4	...
F 2s	−40.0	−31.4	...

^{a} See ref. 83 and 86. ^{b} See ref. 98 and 99. ^{c} See ref. 21 and 23.

Further, the proportionality parameter $K(i,j)$ was taken to be determined by the arithmetic or geometric mean of the Coulomb integrals

$$K(i,j) = (1/2)g(\alpha(i) + \alpha(j))$$

or   (Eq. 17b)

$$K(i,j) = g(\alpha(i)\alpha(j))^{1/2}$$

Various values of the constant g in the region 1.16 to 2.0 were used. This procedure is common in the semiempirical treatment of aromatic molecules and inorganic transition metal compounds.

Some justification for this representation of the exchange integrals is proved by the Mulliken approximation (115). Note that now calculations within the semiempirical molecular orbital scheme described have been reduced to the evaluation of overlap integrals (Table VIII).

TABLE VIII

OVERLAP INTEGRALS FOR MOLECULAR CALCULATIONS FOR XeF_2 AND XeF_4.^{a}

Integral	R, a.u.	S
$S(\text{Xe } p\sigma_z, \text{F } p\sigma1_z)$	3.78	0.1675
$S(\text{Xe } p\pi_z, \text{F } p\pi1_z)$	3.78	0.04696
$S(\text{F } p\sigma1_z, \text{F } p\sigma2_y)$	5.34	0.01157
$S(\text{F } p\sigma1_z, \text{F } p\sigma2_z)$	5.34	0.01771

^{a} Phase convention as in Table VI.

Table IX

Calculated Ground-State Charge Distribution in the Xenon Fluorides[a]

Molecule	$p\sigma$ orbitals only (86)	$p\sigma$ orbitals + d-contribution (64)	Xe 5s, 5p, 4d F 2s, 2p (99)	ω-method, $p\sigma$ orbitals (86)	ω-method, $p\sigma$ orbitals (96)
XeF_2	0.80	0.30	0.25	0.63	0.58
XeF_4	0.80	0.23	0.25	0.49	0.50
XeF_6					0.44

[a] Excess negative charge on the F atom.

The results of detailed calculations demonstrate that the bonding interactions involve principally $p\sigma$ orbitals. Very small mixing of the Xe(5s), Xe(4d), Xe(6s), and Xe(5d) orbitals was obtained (21, 23, 64, 98, 99). Somewhat larger contributions of the F(2s) orbital have been claimed, but the results depend strongly on the parameters chosen. In the language of the classical chemist, all of the results imply negligible s-$p\sigma$ or dσ-$p\sigma$ hybridization for the xenon atom; the extent of s-p hybridization for the fluorine $p\sigma$ orbitals may be somewhat larger (99), but is still small relative to the ordinary one-to-one mixing.

The calculations cited indicate that there is substantial migration of negative charge from the xenon to the fluorine. As noted earlier, both the bonding and antibonding π-orbitals are filled, and therefore the π-orbitals do not contribute to the charge migration. It is obvious that charge will flow from Xe to F, because the first ionization potentials are 12.12 and 17.42 e.v., respectively. Now, neglecting atomic overlap leads to net charges $(1 + b_-^2)^{-1}$, $2(1 + b_-^2)^{-1}$, and $(1 + b_-^2)^{-1}$, with the F atoms negative (43). If $b_- < 1$, then each F atom carries a net charge of the order of 0.5 of a unit charge (43). It is apparent that the low ionization potential of the central atom and the electronegative character of the ligands (a rather vague concept) are of crucial importance. The xenon fluorides are semiionic compounds, for which a convenient notation is $F^{\delta-} Xe^{2\delta+} F^{\delta-}$ with charges δ as indicated above (43, 86).

The electronegativity of the central xenon atom is expected to increase with increasing charge migration to the ligands. Now, the electronegativity of Xe has been estimated by the Mulliken method to be 2.25 (135, 137). However, for Xe^+ the electronegativity is much larger (43). Within the molecular orbital scheme the effect of the charge redistribution on the Coulomb integrals can be taken into account by the iterative ω-technique (158). The Coulomb integrals are assumed to depend on the net charge on atom i

$$[\alpha(i)]^\mu = [\alpha(i)]^{\mu-1} - (m_i - q_i^{(\mu-1)})\omega \quad \text{(Eq. 37)}$$

where $[\alpha(i)]^\mu$ and $q_i^{(\mu-1)}$ are the Coulomb integral and the negative charge on atom i obtained in the μth iteration. This method is supposed to account semiempirically for interelectronic repulsion. Application of this method (86, 96) to the xenon fluorides shows that

the charge on the F atom should decrease in the sequence $XeF_2 > XeF_4 > XeF_6$.

In Table IX are displayed the results of the theoretical calculations of the charge distribution in the ground state of the xenon fluorides. The results of different authors cannot be directly compared owing to differences in the approximations involved. However, despite quantitative differences, the various treatments show the same trend, so that the general features of the charge migration predicted by the theory may be trusted despite the semiempirical elements inherent in the analysis. The comparison of the theoretical charge distribution with experimental data, which will be reviewed in a later section, shows that the results of the ω-technique are in good agreement with the n.m.r. data for these compounds (63, 96).

E. THE VALENCE BOND MODEL

In the valence bond model, molecular wave functions are constructed from the wave functions of the individual atoms. Indeed, valence bond wave functions can be constructed from xenon hybrid orbitals which are used to form electron pairs with the fluorine $2p\sigma$ orbitals. For XeF_2 the two p^3d^2s orthogonal diagonal hybrids (15)

$$\text{Xe di}_{1,2} = \frac{1}{\sqrt{6}}(\text{Xe 5s}) \mp \frac{1}{\sqrt{2}}(\text{Xe 5p}\sigma) + \frac{1}{\sqrt{3}}(\text{Xe 5d}_{z^2}) \quad \text{(Eq. 38)}$$

are used. The wave functions corresponding to the following structures have been considered (15)

$$\Psi_{cov}(FXeF) = \frac{1}{2} \sum_R (-)^R R \left(\frac{1}{4!}\right)^{1/2} \sum_P (-)^P P \times$$
$$[\text{Xe di}_1(1)\overline{F_1\ 2p\sigma(2)}\text{Xe di}_2(3)\overline{F_2\ 2p\sigma(4)}]$$

$$\Psi_{Xe^+}(FXe^+F^-) = \frac{1}{2} \sum_R (-)^R R \left(\frac{1}{4!}\right)^{1/2} \sum_P (-)^P P \times$$
$$\frac{1}{\sqrt{2}}\ [\text{Xe di}_1(1)\overline{F_1\ 2p\sigma(2)}F_2\ p\sigma(3)\overline{F_2\ 2p\sigma(4)} +$$
$$F_1\ 2p\sigma(1)\overline{F_1\ 2p\sigma(2)}\text{Xe di}_2(3)\overline{F_2\ 2p\sigma(4)}]$$

$$\Psi_{Xe^{+2}}(F^-Xe^{+2}F^-) =$$
$$\frac{1}{\sqrt{4!}} \sum_P (-)^P P [F_1\ 2p\sigma(1)\overline{F_1\ 2p\sigma(2)}F_2\ 2p\sigma(3)\overline{F_2\ 2p\sigma(4)}]$$
$$\text{(Eq. 39)}$$

The operators R and P permute the spins of bond partners and the electron coordinates, respectively. The state function is then represented by a linear combination of the states Ψ_{cov}, Ψ_{Xe^+}, and $\Psi_{Xe^{+2}}$, with the linear combination coefficients expressed in terms of the "p-electron defect", i.e., the number of electrons removed from the Xe $5p\sigma$ orbital. It has been suggested (15) that the p-electron defect can be estimated from quadrupole coupling data. A similar treatment of localized pairs formed from p^3d^2s hybrids has also been used for the calculation of chemical shifts. As mentioned earlier, these models are not satisfactory, since hybrid orbital formation involves too much promotion energy, and the contribution of Xe 5s and 5d orbitals to the bonding is expected to be small.

Another version of the valence bond model involves a qualitative discussion in terms of Pauling resonance structures (43, 156). For XeF_2 the resonating structures F^-Xe^+-F and $F-Xe^+F^-$ are considered. It is assumed, again, that the bonding is due to $p\sigma$ orbitals. If the bonds are covalent, the xenon atom will carry a unit positive charge. The addition of the structure $\overline{FXeF}$ reduces this charge migration, while inclusion of the structure $F^-Xe^{+2}F^-$ will increase it (43). On the basis of electronegativity arguments, the charge distribution in the xenon difluoride is estimated to be $F^{-1/2}Xe^+F^{-1/2}$, in agreement with the prediction of the molecular orbital scheme.

A more elaborate valence bond analysis of XeF_2, considering four electrons from the $2p\sigma$ orbitals of the fluorine atoms and the $5p\sigma$ orbital on the Xe atom, has been made (16). The four structures of the correct symmetry are (16)

$$\Psi_1(\overline{FXeF}) = \sum_P (-)^P P \times$$

$$[F_1\,2p\sigma(1)\overline{Xe\,5p\sigma(2)}Xe\,5p\sigma(3)\overline{F_2\,2p\sigma(4)} +$$

$$F_2\,2p\sigma(1)\overline{Xe\,5p\sigma(2)}Xe\,5p\sigma(3)\overline{F_1\,2p\sigma(4)}]$$

$$\Psi_2(FXe^+F^-) = \sum_P (-)^P P \times$$

$$[F_1\,2p\sigma(1)\overline{Xe\,5p\sigma(2)}F_2\,2p\sigma(3)\overline{F_2\,2p\sigma(4)} +$$

$$Xe\,5p\sigma(1)\overline{F_1\,2p\sigma(2)}F_2\,2p\sigma(3)\overline{F_2\,2p\sigma(4)} +$$

$$F_1\,2p\sigma(1)\overline{F_1\,2p\sigma(2)}Xe\,5p\sigma(3)\overline{F_2\,2p\sigma(4)} +$$

$$F_1\,2p\sigma(1)\overline{F_1\,2p\sigma(2)}F_2\,2p\sigma(3)\overline{Xe\,5p\sigma(4)}] \quad (Eq.\ 40)$$

$$\Psi_3(F^+XeF^-) = \sum_P (-)^P P \times$$

$$[F_1\,2p\sigma(1)\overline{F_1\,2p\sigma(2)}Xe\,5p\sigma(3)\overline{Xe\,5p\sigma(4)} +$$

$$Xe\,5p\sigma(1)\overline{Xe\,5p\sigma(2)}F_2\,2p\sigma(3)\overline{F_2\,2p\sigma(4)}]$$

$$\Psi_4(F^-Xe^{+2}F^-) = \sum_P (-)^P P \times$$

$$[F_1\,2p\sigma(1)\overline{F_1\,2p\sigma(2)}\,F_2\,2p\sigma(3)\,\overline{F_2\,2p\sigma(4)}]$$

The molecular integrals used for the configuration interaction scheme were estimated by semiempirical methods, and the final wave function obtained is (16)

$$\Psi_{vb} = 0.223\Psi_1 + 0.270\Psi_2 + 0.039\Psi_3 + 0.547\Psi_4$$

$$(Eq.\ 41)$$

The calculated energy was compared with the energies calculated from approximate wave functions (where the integrals were computed in the same way) (16). The MO function $(a_{2u})^2(a_{1g})^2$ and the Heitler–London bond orbitals lead to energies which are higher than that corresponding to Ψ_{vb} by 0.66 and 1.30 e.v., respectively. The energy of an unpaired split orbital (16) function represented by the formula $\dot{F}\cdot Xe\cdot\dot{F}$ (based on the electronic configuration $(F_1\,2p\sigma)[(F_1\text{-}2p\sigma) + k(Xe\,5p\sigma)][(k(Xe\,5p\sigma) + (F_2\,2p\sigma)](F_2\,2p\sigma)$ is very close to the configuration interaction energy. The best value for the parameter k was found to be 0.92, confirming again the gross features of the charge distribution predicted by other methods.

It should be noted that in the valence bond approximation, the only contributing structures are ionic. Although this set of structures is correct, similar situations have not often been encountered before (43, 44).

Configuration interaction between the structures (1) $F_1\,2p\sigma\,(Xe\,5p\sigma)^2\,F_2\,2p\sigma$, (2) $(F_1\,2p\sigma)^2\,(Xe\,5p\sigma)^2$, (3) $(F_2\,2p\sigma)^2\,(Xe\,5p\sigma)^2$, and (4) $(F_1\,2p\sigma)^2\,(F_2\,2p\sigma)^2$, is analogous to the treatment of the super-exchange mechanism in antiferromagnetic oxides such as MnO (7). In these insulators, the magnetic ions are separated by a closed-shell ligand, the ground-state configuration being $Mn^{+2}O^{-2}Mn^{+2}$. An important contribution to the interaction between the paramagnetic ions arises from the following possibility (7, 120). A pair of electrons in a single, doubly filled ligand orbital φ_1 are excited simultaneously, one into a spin-up orbital and the other into a spin-down orbital on the ions m and m′, respectively. This effect amounts to configuration interaction between configurations which differ by two occupied orbitals. Also, there can be a drift of an electron from one paramagnetic ion to the other (7). Now, these two contributions to the super-exchange effect are analogous to the configuration interaction between the four structures of XeF_2 listed above, where the Xe atom replaces the ligand and the two fluorine atoms replace the paramagnetic ions (121). Within the framework of the second-order perturbation theory (120, 121), the binding energy (per XeF bond) is given by

$$\langle[Xe\,5p\sigma(1)][F_1\,2p\sigma(1)]|r_{12}^{-1}|[Xe\,5p\sigma(2)] \times$$

$$[F_2\,2p\sigma(2)]\rangle^2\left(\frac{1}{E_4} + \frac{1}{E_2}\right) \quad (Eq.\ 42)$$

where E_4 is the energy of configuration 4 relative to 1, and E_2 is the energy of configuration 2 or 3 relative to 1.

TABLE X

MOLECULAR GEOMETRY AND BOND LENGTHS PREDICTED FOR XeF_2 AND XeF_4 BY THE MO METHOD

Molecule	Symmetry	R_{Xe-F} (calcd.),[a] Å.	R_{Xe-F} (exptl.), Å.	Calculated bond energy, e.v.	Atomic orbital set	Ref.
XeF_2	$D_{\infty h}$ (linear)	2.4	2.0	3.3	F 2s, 2p Xe 5s, 5p, 4d	99
	$D_{\infty h}$	1.85	2.0	3.7	pσ orbitals ω technique	86
	$D_{\infty h}$	1.90	2.0	5.6	pσ orbitals only	86
	C_{2v} (bond angle 120°)	(2.4)	...	2.6	F 2s, 2p Xe 5s, 5p, 4d	99
	C_{2v} (bond angle 90°)	(2.4)	...	1.8	F 2s, 2p Xe 5s, 5p, 4d	99
XeF_4	D_{4h} (square-planar)	2.4	1.95	3.4	F 2s, 2p Xe 5s, 5p, 4d	99
	D_{4h}	1.85	1.95	5.7	pσ orbitals only	86
	C_{4v} (bond angle 70° 32′)	(2.4)	...	2.4	F 2s, 2p Xe 5s, 5p, 4d	99
	C_{2v} (bond angle 90°)	(2.4)	...	2.7	F 2s, 2p Xe 5s, 5p, 4d	99
	T_d (tetrahedral)	(2.4)	...	2.4	F 2s, 2p Xe 5s, 5p, 4d	99

[a] For the bond distances in parentheses, the bond energy was not minimized with respect to the Xe–F distance.

The several E_i may be estimated by use of a point-charge electrostatic model, whereupon, (121)

$$E_4 = I^1_{Xe} + I^2_{Xe} - 2A_F - 50.40/d \quad \text{(e.v.)}$$

$$E_2 = I_F - A_F - 7.20/d$$

(Eq. 43)

where I^1_{Xe}, I^2_{Xe}, and I_F are the first and second ionization potentials of xenon and the ionization potential of F, respectively, and d is the Xe–F bond length. This model exhibits the dependence of the binding energy in the linear rare gas dihalides on the ionization potential of the rare gas atom and on the size of the ligand. Unfortunately, the exchange integral is used as an empirical parameter to obtain agreement with experiment. The value chosen (121) for the exchange integral ($\sim$1 e.v.) is about one order of magnitude larger than that observed in antiferromagnetic oxides (7). The model is limited to only the symmetric dihalides. A comparison of the results of the super-exchange model with the Coulomb integral valence bond wave function indicates that the former seems to underestimate the effects of ionic structures. This difficulty may arise from the restrictions imposed by strict adherence to the structures encountered in super-exchange and the neglect of important configurations such as FX^+F^-. Also, the use of perturbation theory within the valence bond scheme is questionable.

It is interesting to compare the predictions of the valence bond and the molecular orbital models. The determinantal wave function for XeF_2 corresponding to the MO description $(a_{2u})^2(a_{1g})^2$ may be expanded and terms grouped together so that they may be identified with terms corresponding to the various valence bond structures. This analysis gives (43) (using the notation of Eq. 41)

$$\Psi(a_{2u}{}^2 a_{1g}{}^2) = \frac{\lambda^2}{2\sqrt{2}}\Psi_1 + \frac{\lambda}{\sqrt{2}}\Psi_2 + \frac{\lambda^2}{4}\Psi_3 + \Psi_4$$

(Eq. 44)

where $\lambda = \sqrt{2}b_-/a_- \approx 0.6$. The ratios of the coefficients are $0.12:0.41:0.09:1$; these ratios should be compared with the ratios obtained from the valence bond wave function (Eq. 41) $0.15:0.13:0.07:0.55$. It is apparent that the MO scheme overemphasizes the contribution of ionic terms, a common state of affairs (44). The obvious disadvantage of the valence bond scheme is that any discussion of excited electronic states is much more difficult than in the MO theory.

VII. INTERPRETATION OF PHYSICAL PROPERTIES

The experimental techniques employed to elucidate the structure and the ground-state charge distribution in xenon compounds include X-ray and neutron diffraction, infrared and Raman spectroscopy, studies of magnetic properties, n.m.r. and e.p.r. spectroscopy, and Mössbauer effect studies. Information regarding the excited states of these molecules is obtained from near-ultraviolet and vacuum-ultraviolet spectroscopy. There now remains the important task of discussing the observed properties in terms of the theoretical models. In this discussion either the molecular orbital or the valence bond model will be used, as is appropriate.

A. MOLECULAR GEOMETRY OF THE XENON FLUORIDES

Structural data for solid XeF_2 and XeF_4 (30, 97, 144, 145, 156, 163) and the infrared and Raman spectra of these compounds (38, 39, 152–154) demonstrate that the ground state of XeF_2 is linear (symmetry $D_{\infty h}$) while that of XeF_4 is square-planar

TABLE XI

N.M.R. DATA FOR THE RARE GAS FLUORIDES[a]

Compound	$10^6 \Delta \sigma_F$		$10^4 \Delta \sigma_{Xe}$		J_{Xe-X}, c.p.s.
	Theor.	Exptl.	Theor.	Exptl.	(exptl.)
XeF_2	462	629	−4160	−3930	5690 (X = F)
XeF_4	400	450	−5400	−5785	3864 (X = F)
XeF_6	352	310	−5320	...	...
KrF_4[b]	334	370	...	...	...
$XeOF_4$	...	317	...	...	692 (X = O[17])

[a] Theoretical values from ref. 96. [b] NOTE ADDED IN PROOF.—Recent work by Schreiner, Malm, and Hindman shows that the entries for KrF_4 actually refer to KrF_2.

(symmetry D_{4h}). These results can be rationalized by the semiempirical MO treatment (Table X). Although the bond energies (58, 157) are seriously overestimated, the relative stability of the various nuclear configurations is expected to be faithfully reproduced by the theory. Minimization of the bond energy with respect to the Xe–F separation leads to predicted bond lengths in fair agreement with experiment (86, 98, 99).

The molecular orbital scheme predicts (21, 99) that the ground state of XeF_6 is a regular octahedron (symmetry group O_h). The infrared spectrum of the gaseous compound and the Raman spectrum of the solid seem to rule out this high symmetry (152).

B. ELECTRON SPIN RESONANCE SPECTRUM OF XeF (113)

The radical XeF has been prepared by γ-irradiation of a single crystal of XeF_4 (49). An e.s.r. study of the oriented radical (113) provides information concerning the s- and p-character of the orbital of the unpaired electron. The hyperfine splittings due to the nuclei F^{19}, Xe^{129}, and Xe^{131} were found to be very large, so that second-order terms in the hyperfine interactions must be retained in the spin-Hamiltonian (113). For the $Xe^{132}F$ radical, the interaction is of one nucleus with spin $1/2$, leading to a two-line spectrum. The hyperfine interaction for $Xe^{129}F$ is that of two nuclei of spin $1/2$, resulting in a four-line spectrum, while for $Xe^{131}F$, interactions with nuclei of spin $3/2$ and $1/2$ lead to an eight-line spectrum. The principal values of the F^{19} and Xe^{129} hyperfine-interaction tensors have been resolved into isotropic components, $A_F = 1243$ and $A_{Xe} = 1605$ Mc., and into the anisotropic components, $B_F = 703$ and $B_{Xe} = 382$ Mc. Neglecting inner-shell polarization effects, the isotropic factor A is determined by the contributions of the atomic s-orbitals to the molecular orbital of the unpaired electron. A_F is the measure of the unpaired electron spin density at the fluorine nuclei, i.e.

$$A_F = \frac{8\pi g\beta\gamma}{3h} |u_{F\ 2s}(0)|^2 C^2_{F\ 2s} = 47,900 C^2_{F\ 2s} \quad \text{(Mc.)}$$

$$A_{Xe} = \frac{8\pi g\beta\gamma}{3h} |u_{Xe\ 5s}(0)|^2 C^2_{Xe\ 5s} = 33,030 C^2_{Xe\ 5s} \quad \text{(Mc.)}$$

(Eq. 45)

where β is the Bohr magneton, γ is the gyromagnetic ratio of the nucleus, $C^2_{F\ 2s}$ and $C^2_{Xe\ 5s}$ represent the F (2s) and the Xe(5s) population of the unpaired MO, and the $|u(0)|^2$ values are the atomic spin densities of the corresponding orbitals on the nuclei. The analysis leads to $C^2_{F\ 2s} = 0.026$ and $C^2_{Xe\ 5s} = 0.049$.

The anisotropic components of the hyperfine interaction tensors arise from electron spin–nuclear spin interactions and depend on the value of $\langle r^{-3} \rangle_{np}$, the inverse mean-cube-distance of an electron from the nucleus (obtained from atomic data). The anisotropic components, B, may be represented in the form

$$B_F = \frac{2g\beta\alpha}{h} \langle r^{-3} \rangle_{F\ 2p} C^2_{F\ 2p} = 1515 C^2_{F\ 2p}$$

(Eq. 46)

$$B_{Xe} = \frac{2g\beta\alpha}{h} \langle r^{-3} \rangle_{Xe\ 5p} C_{Xe\ 5p} = 1052 C^2_{Xe\ 5p}$$

The experimentally determined values for the $np\sigma$ population of the xenon and fluorine orbitals are $C^2_{Xe\ 5p} = 0.36$ and $C^2_{F\ 2p} = 0.47$. The experimental departures of the principal g-values from the free-spin values are associated with spin-orbit coupling between the σ-orbital and excited π-orbitals. These changes are consistent with the p-population analysis.

These experiments demonstrate that the unpaired electron in the XeF radical occupies a σ-antibonding orbital of chiefly F $2p\sigma$ and Xe $5p\sigma$ character, i.e., $\sigma = a(\text{F } 2p\sigma) - b(\text{Xe } 5p\sigma)$, with $a^2/b^2 \approx 1.3$. The s-character of this orbital is small. This result is in agreement with the molecular orbital treatment regarding the canonical contributing orbitals involved in the binding. Furthermore, the charge distribution in the XeF radical is adequately accounted for by the MO scheme.

C. NUCLEAR MAGNETIC RESONANCE STUDIES

Several n.m.r. studies of the xenon fluorides in the solid state and in HF solution have been published (17, 18, 25–28, 63, 73, 104, 136). The available experimental results include the Xe^{129} chemical shifts $\Delta\sigma_{Xe}$ (with respect to atomic Xe), the F^{19} chemical shifts $\Delta\sigma_F$ (with respect to liquid HF or to gaseous F_2), and the Xe–F coupling constants J_{Xe-F} (Table XI). Environmental and temperature effects on the chemical shift of XeF_6 were found to be negligible. XeF_2 and

XeF_6 were found to undergo exchange with the HF solvent, with resultant broadening of the resonances (63). Spin-lattice relaxation times in solid XeF_4 have also been studied (167).

A semiquantitative treatment of the chemical shifts can be given within the framework of the molecular orbital scheme (96). The paramagnetic contribution $\sigma^{(2)}$ to the nuclear shielding, which is expected to dominate the Xe and F chemical shifts, is approximated by (nucleus A is Xe or F)

$$\sigma_A^{(2)} = -\frac{2e^2\hbar}{3mc^2\Delta E^A}\left\langle\frac{1}{r^3}\right\rangle_A [p_{zz}^A + p_{yy}^A + p_{zz}^A - \frac{1}{2}(p_{zz}^A p_{yy}^A + p_{yy}^A p_{zz}^A + p_{zz}^A p_{zz}^A)] \quad \text{(Eq. 47)}$$

where p_{ii}^A represents the atomic population of the valence shell pσ orbital of atom A, calculated by the MO method, $\langle 1/r^3\rangle_A$ the mean inverse cube of the distance of an electron from the nucleus in this orbital, and ΔE^A the average excitation energies estimated from spectroscopic data. The ω-type MO scheme accounts for the trends observed in the chemical shifts (96) $\Delta\sigma_{Xe}(XeF_4) > \Delta\sigma_{Xe}(XeF_2)$ and $\Delta\sigma_F(XeF_2) > \Delta\sigma_F(XeF_4) > \Delta\sigma_F(XeF_6)$, which demonstrate the decrease of charge migration in the series XeF_2, XeF_4, and XeF_6.

The shielding anisotropy in XeF_4 has recently been found to be $\sigma_\perp^F - \sigma_\parallel^F = -570 \pm 40$ p.p.m. (19), in good agreement with the theoretical value -800 p.p.m. obtained from the same model (87).

An alternative treatment of the chemical shifts has been presented in terms of localized orbitals involving p^3ds, p^3d^2s, and ps xenon hybrid orbitals (79). Unfortunately, such an analysis is not wholly satisfactory because the formation of these hybrid orbitals requires considerable promotion energy, or in MO language, the mixing coefficients for the Xe 4d and 5s orbitals are overestimated. It should be noted, however, that, although the delocalized MO scheme involving pσ orbitals only properly accounts for the chemical shifts in the xenon fluorides, it incorrectly predicts coupling constants J_{XeF} of zero (87). The contribution of the contact term to the spin coupling is expected to be dominant, so that (78)

$$J_{ij} \propto |u_i(0)|^2 |u_j(0)|^2 \quad \text{(Eq. 48)}$$

The observed coupling constants J_{XeF} imply that the contributions of the orbitals Xe 5s and F 2s (although being relatively small) must be included (79). A similar situation arises in the analysis of the vibronically induced electronic transition in the xenon fluorides (131).

D. THE MAGNETIC SUSCEPTIBILITY OF XeF₄

The magnetic susceptibility of XeF_4 has been determined (103, 104) to be $\chi = -50.6 \times 10^{-6}$ e.m.u./mole at 300°K. (the negative sign referring to the fact that the molecule is diamagnetic). Although

preliminary measurements seemed to show a temperature dependence of χ, later experiments established (104) that the susceptibility is temperature independent in the region 100 to 300°K.

A theoretical treatment of the magnetic susceptibility of XeF_4 has been presented in the molecular orbital scheme including the 5p, 5d, 6s, and 6p orbitals of Xe and the 2p orbitals of fluorine (22). The observed magnetic susceptibility was represented as the sum of the diamagnetic contribution χ^D calculated from the Pascal constants and the temperature-independent paramagnetic contribution χ^{FH}. The high-frequency term is related (22) to the matrix elements of the orbital angular momentum operator $\mathbf{m} = \sum_i (e/2mc)\mathbf{l}_i$ connecting the ground state $|0\rangle$ with one-electron excited states $|n\rangle$

$$\chi^{FH} = (2/3)N\sum_{n\neq 0}\frac{\langle 0|\mathbf{m}|n\rangle^2}{E_0 - E_n} \quad \text{(Eq. 49)}$$

where N is Avogadro's number.

The parallel component of the high frequency term $\chi_\parallel^{FH}$ was found to be one order of magnitude smaller than the perpendicular component, $\chi_\perp^{FH}$. The major contribution to $\chi_\perp^{FH}$ arises from a small amount of Xe(5d) mixing; the corresponding contribution of the Xe(5d) orbitals to $\chi_\parallel^{FH}$ is relatively small (about 25%). Since the anisotropy of the magnetic susceptibility has not been determined, only an average value of $\chi^{FH} = 16 \times 10^{-6}$ e.m.u./mole is derived. Combining this result with the calculated value $\chi^D = -69.2 \times 10^{-6}$ e.m.u. leads to a reasonable theoretical estimate of the magnetic susceptibility (22). In view of the small contribution of $\chi_\perp^{FH}$ it is difficult at present to determine the contribution of d-orbital mixing. Determinations of the anisotropy of the magnetic susceptibility will provide useful information concerning the small contribution of the d-orbitals to the binding.

E. THE MÖSSBAUER EFFECT IN THE XENON FLUORIDES

The Mössbauer effect has been employed to study the ground-state charge distribution in compounds of xenon (35, 124). The xenon hydroquinone clathrate and the perxenate ion show a single line unshifted from the zero-velocity line. This is not surprising for the former case since the binding in the clathrate is due to dispersion (and perhaps charge-transfer) interactions. In the perxenate ion, no quadrupole splitting is expected because of the cubic environment. XeF_2 and XeF_4 exhibit a large quadrupole splitting of the Xe^{129} nucleus (41.9 ± 1.1 mm./sec.) and show no isomer shift. These results have been rationalized in terms of the binding scheme involving Xe 5pσ orbitals. The field gradient in XeF_4, eq, is attributed to a doubly occupied Xe $5p_z$ orbital; the charge distribution in the

binding $5p_x$ and $5p_y$ orbitals is assumed not to contribute to the field gradient. The field gradient due to two $5p_z$ electrons is

$$eq = -(8/5)e\left\langle \frac{1}{r^3} \right\rangle \qquad \text{(Eq. 50)}$$

In linear XeF_2 the charge of the two electrons along the bonding axis is assumed to be ineffectual and the gradient due to the remaining four p-orbitals gives the same result, with opposite sign. The quadrupole splitting δq is (35, 124)

$$\delta q = \frac{e^2 qQ}{2} \qquad \text{(Eq. 51)}$$

In the original work it was assumed that the quadrupole moments of the Xe^{129} and the Xe^{131} nuclei are equal. New data (124) show that $Q(Xe^{129})/Q(Xe^{131}) = 3.45 \pm 0.09$. Hence the calculated quadrupole splitting in XeF_2 and XeF_4 is 54.2 mm./sec. (compared with the experimental value of 42 mm./sec.). The calculated splitting is overestimated because the completely ionic model is inadequate. If the partial charge transfer from the Xe atom in XeF_4 is included, the formal charge on each fluorine atom is of the order of 0.75. The assumption made regarding the small contribution of excess charge on the fluorine atoms to the quadrupole splitting may not be valid.

Some experiments have been performed on the quadrupole splitting in XeO_3 and XeO_4 produced by β decay of sodium periodate, $NaI^{129}O_3$, and sodium paraperiodate, $Na_3H_2I^{129}O_6$ (124). The compounds thus formed have lifetimes longer than 10^{-9} sec. No splitting was observed for XeO_4, so that the xenon atom is expected to be located in a cubic environment. For XeO_3 the observed splitting of 11.6 ± 0.6 mm./sec. is consistent with 50% electron transfer from the xenon 5p orbitals to the oxygen atoms. This experiment provides further evidence for charge migration in the ground state of the xenon fluorides and oxides.

F. THE HEATS OF SUBLIMATION OF THE SOLID XENON FLUORIDES

Crystalline XeF_2 and XeF_4 are characterized by high heats of sublimation (12.3 kcal./mole for XeF_2 and 15.3 kcal./mole for XeF_4) (84, 86). We would not expect dispersion and repulsive overlap forces alone to lead to these large heats of sublimation; therefore, other contributions to the heat of sublimation, ΔH_{subl}, must be considered. The proposed models for the binding of the xenon fluorides show substantial charge migration from the xenon to the fluorine, such that the effect of electrostatic interactions on the heat of sublimation has to be considered. Long-range intermolecular interactions in the XeF_2 crystal can be adequately described by (weak) quadrupole-quadrupole forces, but the interaction between near neighbors is better described by the interaction between point charges located at the xenon and fluorine atoms. The computed electrostatic stabilization of the solid, XeF_2, is found to be (84)

$$\Delta H_{subl} = 4.52 q_F^2 \text{ kcal./mole} \qquad \text{(Eq. 52)}$$

where q_F is the charge on the fluorine atom. Using the value of q_F obtained from the MO model for XeF_2, the electrostatic stabilization energy is 11.31 kcal./mole. Thus, the dominant contribution to the stability of crystalline XeF_2 (and XeF_4) arises from electrostatic interactions.

VIII. EXCITED ELECTRONIC STATES

The molecular orbital scheme is extremely useful in the interpretation of the excited electronic states of the xenon fluorides. Indeed, the combination of symmetry considerations with estimates of the orbital energies allows a plausible description of the excited states. In particular, the molecular orbital model allows an estimate of the types and nature of the optical transitions expected in these molecules. The ground-state configuration of XeF_2 (symmetry group $D_{\infty h}$) is (43, 86, 99, 181) $(a_{2u}^-)^2(e_{1u})^4(e_{1g})^4(a_{1g})^2(e_{1u})^4$ and that of XeF_4 (symmetry group D_{4h}) (23, 85, 86, 99) $(e_u)^4(a_{1g})^2(b_{2g})^2(a_{2u})^2(b_{2u})^2(e_g)^4(e_u)^4(a_{2g})^2(b_{1g})^2(a_{2u})^2$. The ground-state configuration of XeF_6 (symmetry group O_h) is (22) $(1t_{1u})^6(1e_{1g})^4(a_{1g})^2$, where in the last case only the σ-type orbitals have been included. Thus, the ground state of each of the three xenon fluorides is expected to be a totally symmetric singlet state, $^1A_{1g}$. The highest-filled molecular orbital for XeF_2 and XeF_4 is a π-type antibonding orbital, while for XeF_6 the highest-filled orbital is expected to be the σ-type a_{1g} nonbonding orbital.

A. ALLOWED ELECTRONIC TRANSITIONS

The first singlet–singlet allowed transition in XeF_2 is from the nonbonding a_{1g} orbital to the antibonding a_{2u} orbital (i.e., $^1A_{1g} \rightarrow {}^1A_{2u}$). The estimated transition energies (taken as the difference of the orbital energies) obtained from the MO model involving a $p\sigma$-type orbitals are 8.1 (86) and 7.5 e.v. (64). A more elaborate MO treatment using Xe 5s, 5p, and 5d orbitals and fluorine 2s and 2p orbitals reduces the difference in the orbital energies to 3.6 e.v. (98). This transition is polarized along the molecular axis (z) (86). In order to evaluate the transition dipole moment, Q, the explicit form of the molecular orbitals is required, so that

$$Q = \sqrt{2}\left\langle \frac{1}{\sqrt{2}}(F \ p\sigma 1 + F \ p\sigma 2)\right| z \left| \times \right.$$

$$\left. \frac{a_+}{\sqrt{2}}(F \ p\sigma 1 - F \ p\sigma 2) + b_+(Xe \ p\sigma) \right\rangle \qquad \text{(Eq. 53)}$$

Table XII

Assignment of the Electronically Excited States of the Xenon Fluorides

Molecule	Transition		$h\nu$ (exptl.),[a] e.v.	$h\nu$ (calcd.),[b,c] e.v.	f_{exptl}	f_{calcd}
XeF$_2$	$^1A_{1g} \rightarrow {}^1E_{1g}$	$(e_{1u} \rightarrow a_{2u})$	5.31	...	0.002	0.001
	$^1A_{1g} \rightarrow {}^1A_{2u}$	$(a_{1g} \rightarrow a_{2u})$	7.9	8.1	0.42	1.1
XeF$_4$	$^1A_{1g} \rightarrow {}^1E_g$	$(a_{2u} \rightarrow e_u)$	4.81	...	0.003	0.001
	$^1A_{1g} \rightarrow {}^1E_u$	$(b_{1g} \rightarrow e_u)$	5.43	...	0.009	0.007
	$^1A_{1g} \rightarrow {}^1E_u$	$(b_{1g} \rightarrow e_u)$	6.8	7.4	0.22	...
	$^1A_{1g} \rightarrow {}^1E_u$	$(a_{2g} \rightarrow e_u)$		7.8		
		$(e_g \rightarrow e_u)$	8.3 (sh)	8.2	...	...
	$^1A_{1g} \rightarrow {}^1E_{1u}$	$(b_{2g} \rightarrow e_u)$		8.6		
	$^1A_{1g} \rightarrow {}^1E_u$	$(a_{1g} \rightarrow e_u)$	9.4	9.1	0.8	...
XeF$_6$	$^1A_{1g} \rightarrow {}^1T_{1u}$		(2.5)	0.6	...	...

[a] Experimental data from ref. 84, 86, 108a, 131, and 180. [b] Theoretical data from ref. 86 and 131. [c] The theoretical transition energy is approximated as the difference in orbital energies.

Q is related to the internuclear F–F separation R by (86)

$$Q = \frac{1}{\sqrt{2}} a_+ R + \frac{1}{2} b_+ RS(\text{F } p\sigma, \text{ Xe } p\sigma) \quad \text{(Eq. 54)}$$

Using the value $R = 4.0$ Å. obtained from X-ray data in crystalline XeF$_2$ and the values of a_+ and b_+ obtained from the MO treatment, f (estimated) $= 1.1$ (86). This transition from a nonbonding to an antibonding orbital (84) may be considered to be an intramolecular charge-transfer transition (114), involving charge transfer from the ligands to the central Xe atom (43, 86).

The allowed transitions for XeF$_4$, their polarizations, and respective transition energies are presented in Table XII. Two strongly allowed $\sigma \rightarrow \sigma$ type transitions are expected, i.e., $b_{1g} \rightarrow e_u$ and $a_{1g} \rightarrow e_u$ separated in energy by approximately 4β (F $p\sigma1$, F $p\sigma2$). The symmetry-allowed $\pi \rightarrow \sigma$ transitions $a_{2g} \rightarrow e_u$ and $b_{2g} \rightarrow e_u$ should overlap the two $\sigma \rightarrow \sigma$ type transitions. The $e_g \rightarrow e_u$ transition is expected to be located between the two strong transitions.

How well are these predictions confirmed by the experimental data? We first consider the over-all interpretation of the spectra.

The absorption spectrum of XeF$_2$ is characterized by a weak band followed by a strong absorption band located at 1580 Å., accompanied by a series of sharp bands (86, 181). The absorption spectrum of XeF$_4$ is characterized by two weak bands followed by two strong bands located at 1840 and 1325 Å. (85, 86). The absorption spectrum of XeF$_6$ is characterized by bands at 3300 and 2750 Å. (108a). No vibrational fine structure of the bands is observed (86). This may indicate excitation to dissociative states. However, high resolution experiments are required to clarify this point.

The strong absorption in XeF$_2$ observed at 1580 Å. is assigned to the singlet–singlet $a_{1g} \rightarrow a_{2u}^-$ transition (43, 64, 86). The calculated transition energy and the oscillator strength are in reasonable agreement with the experimental value.

The two allowed transitions in XeF$_4$ separated by 2.6 e.v. have been assigned to $\sigma \rightarrow \sigma$ type transitions (85, 86). The presence of these two bands in XeF$_4$ confirms the hypothesis of the splitting of the a_{1g} and b_{1g} orbitals because of interaction between adjacent F atoms. The 1850-Å. band was (86) assigned to the $b_{1g} \rightarrow e_u$ and the $a_{2g} \rightarrow e_u$ transitions, while the 1325-Å. band is assigned to the $a_{1g} \rightarrow e_u$ and the $b_{2g} \rightarrow e_u$ transitions. The symmetry allowed $\pi \rightarrow \sigma$ type transition, $e_g \rightarrow e_u$, is probably hidden in the asymmetric onset of the $a_{1g} \rightarrow e_u$ transition. In Table XII the experimental transition energies are compared with the results of the semiempirical calculations. It has also been suggested (23) that the 1325-Å. band be assigned to a $\pi \rightarrow \sigma$, $b_{2u} \rightarrow b_{1g}$ transition.

The first spin-allowed electronic excitation in XeF$_6$ has been assigned to an $a_{1g} \rightarrow t_{1u}$ transition (21). The calculated excitation energy (21) (0.6 e.v.) is in disagreement with experiment ($h\nu = 2.4$ e.v.) (108a). These calculations indicate that the a_{1g} orbital is antibonding, whereas it is expected to be nonbonding.

Another potentially interesting feature of the absorption spectrum of XeF$_4$ should be noted (43, 86). Since the excited MO is doubly degenerate (e_u-type), a Jahn-Teller configurational distortion in the excited state is to be expected, with resulting absorption bands exhibiting a doublet peak. The shape of the $a_{1g} \rightarrow e_u$ band may perhaps be caused by such an effect (85). Similar effects may arise in the case of XeF$_6$ where the vacant level is expected to be a triply degenerate t_{1u} MO.

B. Forbidden Electronic Transitions

In the absorption spectra of XeF$_2$ and XeF$_4$, some weak transitions have been observed which can be assigned either to symmetry forbidden or spin forbidden transitions (85, 86, 131, 181).

The intensity expected for the symmetry forbidden transition may be estimated using the Herzberg–Teller theory of vibronically induced transitions (62) and a MO treatment of the excited electronic states. In

the Born–Oppenheimer approximation, the vibronic wave function of a molecule is expressed in the form (62)

$$\Psi_{kj} = \Theta_k(x,q)\Phi_{kj}(q) \qquad \text{(Eq. 55)}$$

where x and q refer to the complete set of coordinates required to specify the locations of all of the electrons and nuclei, respectively. $\Theta_k(x,q)$ is the electronic wave function of the kth electronic state for fixed q, and $\Phi_{kj}(q)$ is the vibrational wave function of the jth vibrational state of the kth electronic state. The coordinates q are taken to be zero at the equilibrium internuclear separation.

The substitution of the right-hand side of Eq. 55 into the general expression for the transition moment, $M_{gi,kj}$, between vibronic states described by the quantum numbers gi,kj gives

$$M_{gi,kj} = \int \Phi_{gi}{}^*(q)M_{gk}(q)\Phi_{kj}(q)\,dq \qquad \text{(Eq. 56)}$$

where

$$M_{gk}(q) = \int \Theta_g{}^*(x,q)m_e(x)\Theta_k(x,q)\,dx \qquad \text{(Eq. 57)}$$

is the variable electronic transition moment, g denotes the ground state, and m_e is the electronic contribution to the electric dipole moment operator. The contribution of the nuclear term to the transition moment operator vanishes by virtue of orthogonality relations. The total transition probability from state g to state k, invoking the quantum-mechanical sum rule, is found to be

$$f_{g \to k} = \frac{8\pi^2 mc}{3h^2 e^2} E_{g \to k} \sum_i B_i \int \Phi_{gi}{}^*(q)M_{gk}{}^2(q)\Phi_{gi}(q)\,dq \qquad \text{(Eq. 58)}$$

where B_i is the Boltzmann weighting factor for vibrational ground state i, and $E_{g \to k}$ represents a mean transition energy.

In the Herzberg–Teller theory it is assumed that the electronic wave function can be expanded in the following form

$$\Theta_k(x,q) = \Theta_k{}^0(x,q) + \sum_s \lambda_{ks}(q)\Theta_s{}^0(x) \qquad \text{(Eq. 59)}$$

where $\Theta_k{}^0(x)$ is the ground-state electronic wave function for the molecule in the equilibrium nuclear configuration, and the summation is over all excited states s. The coefficients cited above are given by perturbation theory in the form

$$\lambda_{ks}(q) = (E_{g \to k} - E_{g \to s})^{-1} \int \Theta_k{}^0(x)H'(q)\Theta_s{}^0(x)\,dx \qquad \text{(Eq. 60)}$$

where $H'(q)$ is the perturbation Hamiltonian. Then, from Eq. 58 and 59

$$M_{gk}(q) = M_{gk}{}^0 + \sum_s \lambda_{ks}(q)M_{gs}{}^0 + \sum_t \lambda_{gt}(q)M_{tk}{}^0 \qquad \text{(Eq. 61)}$$

For the study of forbidden transitions, we are interested in the cases where $M_{gk}{}^0$ vanishes. We also assume that the ground state does not mix appreciably under vibronic perturbation, so that the final summation also vanishes. Equation 61 then reduces to

$$M_{gk}(q) = \sum \lambda_{ks}(q)M_{gs}{}^0 \qquad \text{(Eq. 62)}$$

In order that $M_{gk}(q)$ be nonvanishing, some $\lambda_{ks}(q)$ and $M_{gs}{}^0$ must be nonvanishing. A nonvanishing $M_{gs}{}^0$ requires the purely electronic transition to be allowed under spin and symmetry selection rules. A nonvanishing $\lambda_{ks}(q)$ requires the integral in Eq. 60 to form the basis of a representation which contains at least once the totally symmetric irreducible representation of the group of the molecule. This latter requirement may be used to determine which vibrations are capable of mixing two electronic states of known symmetry.

For small vibrations the perturbation Hamiltonian may be expanded in powers of the nuclear displacement coordinate q. For each normal vibration a, when nonlinear terms are dropped

$$(H'(q))_a = q_a \frac{\partial H}{\partial q_a} \qquad \text{(Eq. 63)}$$

Replacing the effective Hamiltonian, H, by a Coulomb potential and carrying out a transformation from normal to Cartesian coordinates one obtains

$$(H'(q))_a = q_a \sum_i \sum_\sigma z_\sigma \left(\frac{\partial r_\sigma}{\partial q_a}\right)_0 \left(\frac{r_{i\sigma}}{r_{i\sigma}{}^3}\right) \qquad \text{(Eq. 64)}$$

In Eq. 64 the electrons are labeled by i, the nuclei by σ, and $r_{i\sigma}$ is the vector from electron i to nucleus σ. The derivatives $(\partial r_\sigma / \partial q_a)$ are evaluated for the ground state and are the elements of the matrix which transforms from normal coordinates to Cartesian displacement coordinates.

Using Eq. 60, 62, 63, and 64 and carrying out the summation over vibrational levels, the general expression for the oscillator strength of a "forbidden" band may be written in terms of the characteristics of the intense bands from which it borrows intensity

$$f_{gk} = \sum_s f_{g \to s} \frac{E_{g \to k}}{E_{g \to s}(E_{g \to k} - E_{g \to s})^2} \sum_a \coth\left(\frac{h\nu_a}{2kT}\right)(W_{ks})_a{}^2 \qquad \text{(Eq. 65)}$$

where W_{ks} is the vibrational-electronic interaction energy matrix element between the electronic states k and s. For each normal mode of vibration a, the contribution to W_{ks} is given by

$$(W_{ks})_a = \int \Theta_k{}^0(x) \times$$
$$\left[\sum_\sigma \sum_i z_\sigma e^2 \left(\frac{\partial r_\sigma}{\partial q_a}\right)_0 \frac{r_{i\sigma}}{r_{i\sigma}{}^3} \langle Q_a^2 \rangle^{1/2}\right]\Theta_s{}^0(x)\,dx \qquad \text{(Eq. 66)}$$

where $\langle Q_a{}^2 \rangle^{1/2}$ is the root-mean-square displacement of the normal coordinate of the ath normal mode in the zeroth vibrational state of the ground electronic state. The temperature-dependent factor in Eq. 65 arises from the application of the harmonic oscillator approximation to the ground and excited states.

All the terms in Eq. 65 except $(W_{ks})_a$ may be evaluated empirically. When molecular orbital theory is used to represent the electronic wave function, Eq. 66 can be simplified since the expression in brackets is a one-electron operator. The matrix element therefore vanishes if the configurations of $\Theta_k{}^0$ and $\Theta_s{}^0$ differ in more than one molecular orbital. Eq. 66 can then be written in the form

$$(W_{ks})_a = \int \varphi_1(x) \times$$
$$\left[\sum_\sigma z_\sigma e^2 \left(\frac{\partial \mathbf{r}_\sigma}{\partial q_a}\right)_0 \frac{\mathbf{r}_{i\sigma}}{r_{i\sigma}{}^3} \langle Q_a{}^2 \rangle^{1/2} \right] \varphi_2(x) \, dx \quad \text{(Eq. 67)}$$

where φ_1 and φ_2 are the unmatched molecular orbitals in $\Theta_s{}^0$ and $\Theta_k{}^0$. In the actual calculations, Eq. 67 was represented by the interaction energy between a set of dipoles, $\mathbf{u}_\sigma$, defined by

$$\mathbf{u}_\sigma = z_\sigma e \left(\frac{\partial \mathbf{r}_\sigma}{\partial q_a}\right)_0 \langle Q_a{}^2 \rangle^{1/2} \quad \text{(Eq. 68)}$$

and the electron transition density $e\varphi_1\varphi_2$.

In the harmonic oscillator approximation to the vibrational wave function $\langle Q_a{}^2 \rangle^{1/2}$ is found to be

$$\langle Q_a{}^2 \rangle^{1/2} = \frac{h}{8\pi^2\nu_a} \quad \text{(Eq. 69)}$$

The quantities $(\partial \mathbf{r}_\sigma/\partial q_a)$, obtained from a normal coordinate analysis (180), are the elements of the matrix $\mathbf{M}^{-1}\mathbf{B}\dagger(\mathbf{L}^{-1})\dagger$. The elements of the diagonal matrix $\mathbf{M}$ are the relevant atomic masses. $\mathbf{B}$ is the matrix which transforms from Cartesian to symmetry coordinates, and $\mathbf{L}$ is the matrix which transforms from normal to symmetry coordinates. $\mathbf{L}$ is further defined by the following matrix equation (180)

$$\mathbf{L}\dagger\mathbf{FG} = \Lambda\mathbf{L}\dagger$$
$$\mathbf{G} = \mathbf{LL}\dagger \quad \text{(Eq. 70)}$$

where $\mathbf{F}$ and $\mathbf{G}$ refer to Wilson's potential and kinetic energy matrices.

Before proceeding to a discussion of the results of the theoretical analysis, it is pertinent to examine the formal basis for the study of spin forbidden transitions. In the quantum-mechanical treatment of atomic structure both the diagonal and nondiagonal matrix elements of the spin-orbit interaction are of the same order of magnitude, being determined by the spin-orbit coupling parameter

$$\zeta = \frac{e\hbar^2}{2m^2c^2} \int R(r)\left(\frac{1}{r}\frac{\partial V}{\partial r}\right)R(r)r^2 \, dr \quad \text{(Eq. 71)}$$

where $R(r)$ is the radial wave function and V the potential. The parameter ζ is determined from the experimental multiplet splittings in atomic spectra (90). Oscillator strengths and lifetimes of excited states can be accurately reproduced (90) by introduction of an additional parameter which takes into account the difference between the radial wave functions in the singlet and triplet states. The theoretical treatment of singlet–triplet transitions in polyatomic molecules originated with studies of aromatic molecules. In the treatment of intercombination probabilities in the molecular spectra of the xenon fluorides, the spin-orbit coupling matrix elements were reduced to one-center terms which can then be approximated by appropriate parameters derived from atomic spectra (131). This semiempirical treatment is advantageous in view of the lack of knowledge of the appropriate s.c.f. atomic orbitals for the Xe atom.

In molecules characterized by a singlet ground state, the perturbation resulting from spin-orbit coupling leads to mixing of the triplet excited state with some singlet states and thereby to a finite transition probability from the ground state to the excited triplet state. The molecular spin-orbit coupling operator is given by

$$H_{so} = \frac{e\hbar}{4m^2c^2} \sum_i \mathbf{d}(i) \cdot \mathbf{p}(i) \nabla_i V \quad \text{(Eq. 72)}$$

where $\mathbf{d}(i)$ is the Pauli spin operator, $\mathbf{p}$ the linear momentum, ∇_i the gradient operator, and V the potential due to all the nuclei and all the other electrons. The sum is taken over all the electrons. The interaction between the spin of one electron and the orbital motion of the others is neglected, so that the spin-orbit coupling Hamiltonian, H_{so}, can be displayed in the form of a sum of one-electron operators $\mathbf{a}_x$, $\mathbf{a}_y$, and $\mathbf{a}_z$ defined by the relation

$$\mathbf{a}(i) = \nabla_i V \times \nabla_i \quad \text{(Eq. 73)}$$

When the eigenfunctions of the spin-dependent Hamiltonian are employed as zero-order wave functions, the matrix elements of H_{so} between the triplet wave function Ψ_T and a singlet wave function Ψ_S will vanish unless the two configurations differ only in the spin of one electron and in the occupancy number of a single molecular orbital. In addition, a symmetry restriction is imposed: the direct product $\Psi_T \times \Psi_S$ must belong to the same irreducible representation of the molecular point group as one of the spatial components $\mathbf{a}_x$, $\mathbf{a}_y$, or $\mathbf{a}_z$ of the operator H_{so}. Since $\mathbf{a}_x$, $\mathbf{a}_y$, and $\mathbf{a}_z$ transform like the rotation operators R_x, R_y, and R_z, respectively, at least one of the three direct products $R_x \times \Psi_T \times \Psi_S$, $R_y \times \Psi_T \times \Psi_S$, or $R_z \times \Psi_T \times \Psi_S$ must contain the A_{1g} representation.

The singlet function is mixed with the $M_z = 0$ component of the triplet function by $\sigma_z(i)$ and with the $M_z = \pm 1$ triplet components by $\sigma_x(i)$ and by $\sigma_y(i)$.

Carrying out the summation over the electronic spin coordinates and applying the molecular orbital approximation, the molecular spin-orbit coupling matrix elements are reduced to one-electron integrals.

When the separations between the triplet state and the perturbing singlet states are large compared with the off-diagonal matrix elements of H_{so}, the application of perturbation theory is legitimate and the oscillator strength for the spin forbidden transition is given by

$$f_{G \to T} = \sum_s f_{G \to S} \frac{E_{G \to T}}{E_{G \to S}} \frac{\langle \Psi_T | H_{so} | \Psi_s \rangle^2}{(E_{G \to S} - E_{G \to T})^2} \quad \text{(Eq. 74)}$$

where G, T, and S refer to the ground, triplet, and singlet states, respectively. When $\langle \Psi_T | H_{so} | \Psi_S \rangle$ is of the same order of magnitude as $E_{G \to S} - E_{G \to T}$, an intermediate coupling scheme has to be employed.

In the above treatment (131), the spin-orbit perturbation of the ground singlet state by excited triplets was not considered. For the xenon fluorides this mixing is expected to be small.

The procedures which must be used are now clear. Consider first the effects of vibronic coupling in XeF₂ (131). The allowed singlet–singlet transition at 1580 Å., $^1A_{1g} \to {}^1A_{2u}$, corresponds to the transfer of an electron from the a_{1g} molecular orbital (composed mainly of F $2p\sigma$ orbitals) to the nonbonding a_{2u} molecular orbital (composed mainly of the Xe $5p\sigma$ orbital). The symmetry forbidden transition $^1A_{1g} \to {}^1E_{1g}$, corresponding to the excitation of an electron from the e_{1u} molecular orbital to the a_{2u} molecular orbital, would become allowed if the $^1A_{2u}$ and $^1E_{1g}$ excited states were mixed. From the symmetry requirements earlier placed on the perturbation Hamiltonian, mixing of the $^1A_{2u}$ and $^1E_{1g}$ states is possible only by interaction with the doubly degenerate π_u bending vibration of the linear molecule. From detailed calculations based on the molecular orbitals discussed earlier (now including some Xe 5s character in the a_{1g} molecular orbital), it was found that (131) $f(^1A_{1g} \to {}^1E_{1g})_{estd} = 0.001$ at 300°K.

In the case of XeF₄, the absorption band at 1840 Å. ($f = 0.22$) has been ascribed to two singlet–singlet symmetry allowed transitions (86). One represents the transfer of an electron from a σ-type b_{1g} molecular orbital to the antibonding e_u molecular orbital; the other from a π-type a_{2g} molecular orbital to the same e_u molecular orbital. Both of these transitions are of the type $^1A_{1g} \to {}^1E_u$. The second intense band ($f = 0.80$) at 1325 Å. is similarly ascribed to two symmetry allowed singlet–singlet transitions, one representing excitation from the σ a_{1g} molecular orbital and the other from a π-type b_{2g} molecular orbital. Both of these transitions are also described as $^1A_{1g} \to {}^1E_u$. Now, the symmetry forbidden transition $^1A_{1g} \to {}^1E_g$ from the a_{2u} highest-filled molecular orbital to the antibonding e_u molecular

orbital can gain intensity either by mixing the ^1E_g state with the ^1E_u state by either the a_{2u} or b_{1u} out-of-plane normal vibrations, or by mixing the ^1E_g state and the $^1A_{1u} + {}^1A_{2u} + {}^1B_{1u} + {}^1B_{2u}$ state with the two e_u normal vibrations of the square-planar molecule. This treatment leads to $f(^1A_{1g} \to {}^1E_g)_{estd} = 0.001$ at 300°K.

The perturbation treatment outlined earlier may be used to obtain an order of magnitude estimate of the singlet–triplet transition probability in XeF₂. In symmetry group $D_{\infty h}$ of the linear triatomic molecule, a_z and a_y transform like E_{1g} while a_x transforms like A_{2g}. The lowest triplet state of the molecule is expected to be a $^3A_{2u}$ state corresponding to the $a_{1g} \to a_{2u}$ transition. The $^3A_{2u}$ state can be mixed with $^1E_{1u}$ states by a_z and a_y and with $^1A_{1u}$-type states by a_x. It is interesting to note that the mixing of $^3A_{2u}$ with the corresponding $^1A_{2u}$ state is symmetry forbidden, and no intensity borrowing can occur from the strong 1580-Å. band of XeF₂. We consider states arising from excitation to orbitals mainly involving the Xe atom orbitals, as these are expected to lead to the greatest effect. The mixing of the $^3A_{2u}$ state with the singlet Rydberg-type excited states, $e_{1u} \to a_{1g}$ and $e_{1u} \to e_{2g}$, is negligible since the singlet and triplet states differ by the occupation of two orbitals. The Rydberg state $^1E_{1u}$ arising from the excitation $a_{1g} \to e_{1u}$ (Xe 6p) has not been experimentally observed (up to 13 e.v.), and the corresponding excitation energy is expected to be about 15 e.v. The oscillator strength for the singlet–singlet $\sigma \to \pi^*$ type transition is expected to be low (probably π of the order of 10^{-1} to 10^{-2}). The spin-orbit coupling matrix element can be estimated by considering only one-center terms. The transition strength to the $^3A_{2u}$ state due to the intensity borrowing from the E_{1u} (Xe 6p) state is expected to be of the order of 10^{-6}.

Consider now the intensity borrowing from the $^1E_{1u}$ state (due to the $e_{1g} \to a_{2u}$ excitation). The spin-orbit coupling parameter for this mixing contains terms which involve only the contribution of the fluorine atom, and each of the one-center terms can be approximated by $\zeta_F(2p)/2 = 135$ cm.$^{-1}$. The intensity of the singlet–singlet $\pi \to \sigma^*$ type transition is expected to be small. It has not been observed experimentally and is probably masked by the transition to the $^1A_{2u}$ state. A reasonable estimate for the oscillator strength for this singlet–singlet transition is ~ 0.01. Taking the energy difference between the triplet and singlet states as 2 e.v., its contribution to the transition strength of the $^1A_{1g} \to {}^3A_{2u}$ transition is only $\sim 10^{-7}$. This estimate of the contribution does not include the mixing of the Xe 4d orbitals in the a_{1g} and e_{1u} molecular orbitals, which mixing has been shown to be small. A rough estimate indicates that a 10% admixture of d-character leads to a contribution of 10^{-6} to the oscil-

lator strength for the $^1A_{1g} \rightarrow {}^3A_{2u}$ transition. Another singlet–triplet absorption in XeF_2 which should be considered is the $^1A_{1g} \rightarrow {}^3E_{1u}$ transition arising from the excitation $e_{1g} \rightarrow a_{2u}$. Mixing with the $^1A_{2u}$ state is possible. Using the experimental spectroscopic data for the $^1A_{1g} \rightarrow {}^1A_{2u}$ ($f = 0.45$) transition and assuming that the energy separation between the singlet and triplet states is ~ 2 e.v., the expected intensity borrowing will be of the order of 10^{-4}. It should be noted that the $^3E_{1u}$ state can interact with the corresponding $^1E_{1u}$ state. It is found that the spin-orbit coupling parameter is again determined by the F atom spin-orbit coupling, and the transition strength due to intensity borrowing is of the order of 10^{-6} to 10^{-7}.

We conclude that the singlet–triplet transitions in XeF_2, i.e., $^1A_{1g} \rightarrow {}^3A_{2u}$ and $^1A_{1g} \rightarrow {}^3E_{1u}$, should be characterized by a relatively low oscillator strength $f \sim 10^{-4}$. This is a surprising conclusion since it indicates that, in spite of the presence of the heavy atom, the symmetry restrictions imposed and the lack of nearby excited states lead to a low singlet–triplet transition probability.

Study of spin forbidden transitions in XeF_4 requires consideration of an intermediate coupling scheme. The first triplet state in XeF_4 is expected to be a ^3E_u state arising from the transition $b_{1g} \rightarrow e_u$. Consider the symmetry properties of the operators a_z, a_y, and a_z for this molecule. In the symmetry group D_{4h}, a_x and a_y transform like e_g while a_z transforms like b_{2g}. Hence, a ^3E_u state can be spin-orbit coupled with $^1A_{1u}$, $^1A_{2u}$, $^1B_{1u}$, and $^1B_{2u}$ states by a_x and a_y and with ^1E_u states by a_z.

The spin and symmetry allowed transitions in XeF_4 are found to be: (1) $b_{1g} \rightarrow e_u$; (2) $a_{2g} \rightarrow e_u$; (3) $e_g \rightarrow e_u$; (4) $b_{2g} \rightarrow e_u$; (5) $a_{1g} \rightarrow e_u$. The transitions 1, 2, 4, and 5 are $^1A_{1g} \rightarrow {}^1E_u$, while transition 3 is $^1A_{1g} \rightarrow {}^1A_{1u} + {}^1A_{2u} + {}^1B_{1u} + {}^1B_{2u}$. Hence, all these singlet excited states can mix with the ^3E_u state. It is important to notice that in the case of XeF_4, the doubly degenerate triplet state mixes with the corresponding singlet via spin-orbit interaction. As a first approximation configuration interaction can now be disregarded and only the mixing of the ^3E_u and ^1E_u excited states arising from the same configuration considered. The energy separation between these two pure spin states may be rather small (of the order of 1 to 2 e.v.) so that the perturbation treatment used for XeF_2 seems inappropriate, and a variational method is to be preferred. The problem has been studied in the intermediate coupling scheme, and for XeF_4 one finds $f_{estd} = 0.007$ for $^1A_{1g} \rightarrow {}^3E_u$.

In the case of XeF_2, only one weak band is experimentally observed, with $f = 0.002$. Since the expected singlet–triplet transitions were estimated to be extremely weak, the observed band is assigned to the

vibronic transition $^1A_{1g} \rightarrow {}^1E_{1g}$. The calculated strength of the vibronic transition ($f = 0.001$) agrees with this assignment. Vibronically induced spin allowed symmetry forbidden transitions are expected to show a temperature dependence of the oscillator strength. This is the case for the XeF_2 2330-Å. band which shows a temperature increase of $(df/dT) = 0.12\%/deg.$ (131), thereby providing additional evidence for the assignment of this band to a vibronic transition. The case of XeF_4 is more complicated. Two weak bands have been observed, with intensities of $f = 0.009$ and 0.003. The singlet–triplet transition mixes with the corresponding singlet–singlet transition, and its intensity should be enhanced by a heavy atom effect. In the treatment of the spin forbidden transitions in XeF_4, the configuration interaction with higher ^1E_u states was not taken into account. This is not serious as these spin-orbit coupling matrix elements are expected to be mainly determined by the fluorine atom and will thus be small. The results of these calculations show that the singlet–triplet transition in XeF_4 is expected to be about one order of magnitude more intense than the vibronic transitions. This would indicate that the stronger band at 2280-Å. is the singlet–triplet transition $^1A_{1g} \rightarrow {}^3E_u$, and the weaker band at 2580 Å. is the vibronic transition $^1A_{1g} \rightarrow {}^1E_g$. Furthermore, such an assignment is consistent with the fact that the intensities of the vibronic transitions in XeF_2 and XeF_4 are expected to be nearly the same.

The highest-filled orbital in XeF_6 (assuming an octahedral structure for the molecule) is the σ a_{1g} orbital, from which the transition to the first antibonding t_{1u} orbital is symmetry allowed. Thus, a low lying symmetry forbidden transition does not occur in XeF_6. The transition probability for the spin forbidden $^1A_{1g} \rightarrow {}^3T_u$ transition should be relatively high since the excited state is triply degenerate; as in the case of spin forbidden transitions in XeF_4, an intermediate coupling scheme must be used (131). The location of the first triplet state of XeF_6 is unknown. Some anomalies observed in the n.m.r. relaxation times of XeF_6–HF solutions (28) and the observation of an e.s.r. signal in this system (28) were tentatively interpreted in terms of a low-lying triplet state of XeF_6 (56). However, the experimental data are by no means conclusive. In particular, the e.s.r. evidence just indicates the presence of a paramagnetic species (and not a triplet state) which may be due to paramagnetic impurities. The suggestion that a low-lying triplet ^3T_u state of XeF_6 exists (56), which may be thermally populated at room temperature, is of considerable interest. However, the first singlet $^1T_{1u}$ in XeF_6 lies about 2.5 e.v. above the ground state. The hypothesis of a low-lying triplet implies that the splitting between the $^1T_{1u}$ and $^3T_{1u}$ states is 2.5 e.v. (i.e., the exchange integral would be

about 1.2 e.v.). This value seems somewhat high, particularly in view of the known splitting between the $^1E_{1u}$ and $^3E_{1u}$ states in XeF_4, which is only 1.48 e.v. (*i.e.*, the exchange integral is 0.74 e.v.) (131). An experimental study of the temperature dependence of the magnetic susceptibility of XeF_6 should settle this interesting question.

C. RYDBERG STATES

As a final topic in our discussion of the excited states of the xenon fluorides, we consider the higher excited states not heretofore discussed (86, 181). A set of sharp bands observed on the high energy side of the 1580-Å. band of XeF_2 has been observed and assigned to Rydberg states. The highest-filled orbital in XeF_2 is the e_{1u} π-type orbital involving mainly the Xe $5p\pi$ AO. The sharp bands of XeF_2 located at 1425, 1335, 1215, and 1145 Å. are attributed to one-electron excitation from the e_{1u} orbital. The first two bands are due to excitation into s-type Rydberg states. It should be noted that the $^3P_1$ excited states in the xenon atom are located at 1469.6 and 1295.6 Å., respectively. The splitting between the 1425- and 1335-Å. bands in XeF_2 is due to the p-electron spin-orbit coupling of the xenon atom. The bands located at 1215 and 1145 Å. may correspond to d-type Rydberg states. In the case of the xenon atom, the three allowed $5p^6 \rightarrow 5p^55d$ transitions are located at $5d_{1/2}, \lambda = 1250.2$ Å., $5d_{3/2}, \lambda = 1192.0$ Å., and $5d_{3/2}, \lambda = 1068.2$ Å. (112). Alternatively, all the four Rydberg bands observed for XeF_2 may belong to the same series. In the latter case, two series of Rydberg states are expected, split approximately by the p-electron spin-orbit coupling of xenon. The observed bands could be fitted by two series. The energy difference between the two sets is 0.75 e.v., while the spin-orbit coupling in atomic xenon is $^3/_2\zeta = 1.12$ e.v. A reduction of the spin-orbit coupling constant upon molecule formation has previously been encountered in studies of transition metal ions, so this difference is reasonable.

The first ionization potential of XeF_2 was estimated to be 11.5 ± 0.1 e.v. (181), compared to the value 12.12 e.v. for the ionization potential of xenon. Some of the difference between these values may be due to the effect of π-bonding. The result should be compared with the energy of the highest-filled orbital, *viz.*, the antibonding π-orbital (e_{1u}). The semiempirical MO treatment leads to the value of 11.87 e.v. for the e_{1u} orbital energy, in adequate agreement with experiment (86). However, this result is very sensitive to the choice of parameters used in the theory, and agreement with experiment should not be overemphasized.

IX. DISCUSSION OF THE THEORETICAL MODELS

The semiempirical molecular orbital model and the valence bond model are adequate for the qualitative description of the properties of the xenon compounds. The semiempirical molecular orbital model represents a bonding scheme involving mainly $p\sigma$ atomic orbitals. However, for the interpretation of many physical properties (hyperfine interactions, nuclear spin coupling constants, magnetic susceptibility, and vibronic coupling effects), a small admixture of s- and d-orbitals is essential. Several objections can be raised to the semiempirical MO model:

(1) In view of the approximations used regarding cancellation of nuclear attraction and interelectronic repulsion between various atoms, no reliable predictions of the binding energy and of stability can be made. This is, of course, a general defect of any semiempirical model.

(2) The charge distribution predicted on the basis of the simplest model (involving $p\sigma$ orbitals) overestimates the charge migration. The prediction can be refined by the use of a larger basis set, a C.I. scheme, or the semiempirical ω-technique.

(3) The quantitative numerical predictions of the semiempirical method with respect to the order of the energy levels of the several excited states should be accepted with reservation. A similar semiempirical MO method applied to tetrahedral transition metal complexes leads to an incorrect ordering of some of the energy levels, thereby indicating the difficulties involved in applying a deductive approach to the structure of inorganic compounds.

However, to date the semiempirical MO method has proven to be the most versatile and useful approach to the correlation and classification of the properties of the ground and excited states of the xenon compounds.

The valence bond method is still quite limited in its applicability to the interpretation of experimental data. However, this approach provides considerable physical insight into the nature of binding in the rare gas compounds. The charge distributions predicted by both the MO and the valence bond methods for the ground state of the xenon fluorides are quite similar. Both methods predict substantial charge migration from Xe to F. In the MO scheme, this result orginates from the low ionization potential (*i.e.*, Coulomb integral) for the central rare gas atom (86, 127). In the valence bond method the predominant structures are ionic. Indeed, the ionic structures F^-Xe^+F and FXe^+F^- are quite stable (43). The electrostatic energy for the creation of charges Xe^+F^- is roughly $I_{Xe} - A_F - e^2/R = 1.7$ e.v., which is likely to be recovered as the bond Xe^+-F is formed (43). This general argument demonstrates the importance of the low ionization potential of the central atom, the electronegativity of the ligands, and the small size of the ligands in the formation of the rare gas compounds. The advantage of the F atom relative to the other

halogens is due not to its electron affinity but to its smaller size (43). It is unfortunate that at present more profound predictions cannot be made.

Several other qualitative predictions regarding the stability of the rare gas compounds have been published (3, 64, 99, 118, 122, 125, 127, 171). It is generally agreed that the xenon and radon fluorides are expected to be the most stable. It has also been predicted that HeF_2 should be stable (125) by analogy with HF_2^-. However, if we consider the bond in HF_2^- to result from the interaction of a hydride ion, H^-, with two fluorine atoms, the ionization potential of H^- (0.7 e.v.) is so much lower than that of He (25 e.v.) that it is doubtful whether HeF_2 could exist.

The semiionic description of the ground state of the xenon fluorides implies that the octet rule is still preserved, to the satisfaction of the classical chemist. A similar situation arises in the case of the polyhalogen ions, and these ions have served as prototypes in providing qualitative understanding of the binding in the xenon fluorides (86, 99, 125, 127). Note that the binding scheme involving delocalized σ-type orbitals, first applied to electron-deficient molecules such as the boron hydrides, is clearly also extremely useful for the description of electron-rich molecules, such as the polyhalide ions and the rare gas compounds (43).

It is apparent that the binding in the rare gas compounds can be rationalized within the conventional semiempirical schemes of quantum chemistry. No new principles are involved in the understanding of the nature of the chemical bond in these molecules. A complete *a priori* theoretical treatment of these compounds is impossible at present, but this is a general problem inherent to the quantum-mechanical treatment of all complicated molecular systems.

X. References

(1) Agron, P. A., Begun, G. M., Levy, H. A., Mason, A. A., Jones, C. F., and Smith, D. F., *Science*, 139, 842 (1963).
(2) Allen, L. C., *Science*, 138, 892 (1962).
(3) Allen, L. C., *Nature*, 197, 897 (1963).
(4) Allen, L. C., "Noble-Gas Compounds," University of Chicago Press, Chicago, Ill., 1963, p. 317.
(5) Allen, L. C., and Horrocks, W. D., Jr., *J. Am. Chem. Soc.*, 84, 4344 (1962).
(6) Allen, L. C., Clementi, E., and Gladney, H. M., *Rev. Mod. Phys.*, 35, 465 (1963).
(7) Anderson, P. W., "Solid State Physics," Vol. 14, Academic Press, New York, N. Y., 1963, p. 99.
(8) Appelman, E. H., and Malm, J. G., *J. Am. Chem. Soc.*, 86, 2141 (1964).
(9) Appelman, E. H., and Malm, J. G., *J. Am. Chem. Soc.*, 86, 2297 (1964).
(10) Ballhausen, C. J., "Introduction to Ligand Field Theory," McGraw-Hill Book Co., Inc., New York, N. Y., 1962.
(11) Bartlett, N., *Proc. Chem. Soc.*, 218 (1962).
(12) Bartlett, N., and Jha, N. K., "Noble-Gas Compounds," University of Chicago Press, Chicago, Ill., 1963, p. 23.
(13) Bartlett, N., and Rao, R. R., *Science*, 139, 506 (1963).
(14) Bartlett, N., *Endeavour*, 23, 3 (1964).
(15) Bersohn, R., *J. Chem. Phys.*, 38, 2913 (1963).
(16) Bilham, J., and Linnett, J. W., *Nature*, 201, 1323 (1964).
(17) Blinc, R., Podnar, P., Slivnik, J., and Volavšek, B., *Phys. Letters*, 4, 124 (1963).
(18) Blinc, R., Zupančič, I., Maričič, S., and Veksli, Z., *J. Chem. Phys.*, 39, 2109 (1963).
(19) Blinc, R., Zupančič, I., Maričič, S., and Veksli, Z., *J. Chem. Phys.*, 40, 3739 (1964).
(20) Bohn, R. K., Katada, K., Martinez, J. V., and Bauer, S. H., "Noble-Gas Compounds," University of Chicago Press, Chicago, Ill., 1963, p. 238.
(21) Boudreaux, E. A., "Noble-Gas Compounds," University of Chicago Press, Chicago, Ill., 1963, p. 354.
(22) Boudreaux, E. A., *J. Chem. Phys.*, 40, 229 (1964).
(23) Boudreaux, E. A., *J. Chem. Phys.*, 40, 246 (1964).
(24) Brillouin, L., "Le Champs 'Self-Consistent' de Hartree et de Fock," Hermann et Cie, Paris, 1934, p. 19.
(25) Brown, T. H., Whipple, E. B., and Verdier, P. H., *Science*, 140, 178 (1963).
(26) Brown, T. H., Whipple, E. B., and Verdier, P. H., *J. Chem. Phys.*, 38, 3029 (1963).
(27) Brown, T. H., Whipple, E. B., and Verdier, P. H., "Noble-Gas Compounds," University of Chicago Press, Chicago, Ill., 1963, p. 263.
(28) Brown, T. H., Kasai, P. H., and Verdier, P. H., *J. Chem. Phys.*, 40, 3448 (1964).
(29) Burns, J. H., *J. Phys. Chem.*, 67, 536 (1963).
(30) Burns, J. H., Ellison, R. D., and Levy, H. A., *J. Phys. Chem.*, 67, 1569 (1963).
(31) Burns, J. H., Agron, P. A., and Levy, H. A., *Science*, 139, 1209 (1963).
(32) Chernick, C. L., *et al.*, *Science*, 138, 136 (1962).
(33) Chernick, C. L., *Record Chem. Progr.* (Kresge-Hooker Sci. Lib.), 24, 139 (1963).
(34) Chernick, C. L., "Noble-Gas Compounds," University of Chicago Press, Chicago, Ill., 1963, p. 35.
(35) Chernick, C. L., Johnson, C. E., Malm, J. G., Perlow, G. J., and Perlow, M. R., *Phys. Letters*, 5, 103 (1963).
(36) Chernick, C. L., Claassen, H. H., Malm, J. G., and Plurien, P. L., "Noble-Gas Compounds," University of Chicago Press, Chicago, Ill., 1963, p. 106.
(37) Claassen, H. H., Selig, H., and Malm, J. G., *J. Am. Chem. Soc.*, 84, 3593 (1962).
(38) Claassen, H. H., Chernick, C. L., and Malm, J. G., "Noble-Gas Compounds," University of Chicago Press, Chicago, Ill., 1963, p. 287.
(39) Claassen, H. H. Chernick, C. L., and Malm, J. G., *J. Am. Chem. Soc.*, 85, 1927 (1963).
(40) Claassen, H. H., and Knapp, G., *J. Am. Chem. Soc.*, 86, 2341 (1964).
(41) Clifford, A. F., and Zeilenga, G. R., *Science*, 143, 1431 (1964).
(42) Coulson, C. A., and Chirgwin, M., *Proc. Roy. Soc.* (London), A201, 196 (1950).

(43) Coulson, C. A., *J. Chem. Soc.*, 1442 (1964).
(44) Coulson, C. A., "Valence," Oxford University Press, London, 1952.
(45) Daudel, R., Le Fevre, R., and Moser, C., "Quantum Chemistry," Interscience Publishers, Inc., New York, N. Y., 1956.
(46) Dudley, F. B., Gard, G., and Cady, G. H., *Inorg. Chem.*, **2**, 228 (1963).
(47) Edwards, A. J., Holloway, J. H., and Peacock, R. D., *Proc. Chem. Soc.*, 275 (1963).
(48) Edwards, A. J., Holloway, J. H., and Peacock, R. D., "Noble-Gas Compounds," University of Chicago Press, Chicago, Ill., 1963, p. 71.
(49) Falconer, W. E., and Morton, J. R., *Proc. Chem. Soc.*, 95 (1963).
(50) Feder, H. M., Hubbard, W. N., Wise, S. S., and Margrave, J. L., *J. Phys. Chem.*, **67**, 1148 (1963).
(51) Feltz, A., *Z. Chem.*, **4**, 41 (1964).
(52) Ferguson, E. E., and Broida, H. P., *J. Chem. Phys.*, **40**, 3715 (1964).
(53) Fong, K. S., and Hung, S. Y., *Huaxue Tongbao*, 8 (1964).
(54) Gillespie, R. J., "Noble-Gas Compounds," University of Chicago Press, Chicago, Ill., 1963, p. 333.
(55) Gard, G. L., Dudley, F. B., and Cady, G. H., "Noble-Gas Compounds," University of Chicago Press, Chicago, Ill., 1963, p. 109.
(56) Goodman, G. L., see ref. 28.
(57) Gruen, D. M., "Noble-Gas Compounds," University of Chicago Press, Chicago, Ill., 1963, p. 174.
(58) Gunn, S. R., "Noble-Gas Compounds," University of Chicago Press, Chicago, Ill., 1963, p. 149.
(59) Gunn, S. R., and Williamson, S. M., *Science*, **140**, 177 (1963).
(60) Hamilton, W. C., Ibers, J. A., and MacKenzie, D. R., *Science*, **141**, 532 (1963).
(61) Hemmerich, P., *Chimia*, **17**, 289 (1963).
(62) Herzberg, G., and Teller, E., *Z. physik. Chem.* (Leipzig), **B21**, 410 (1933).
(63) Hindman, J. C., and Svirmickas, A., "Noble-Gas Compounds," University of Chicago Press, Chicago, Ill., 1963, p. 251.
(64) Hinze, J., and Pitzer, K. S., "Noble-Gas Compounds," University of Chicago Press, Chicago, Ill., 1963, p. 340.
(65) Hoffman, R., *J. Chem. Phys.*, **39**, 1397 (1963).
(66) Holloway, J. H., and Peacock, R. D., *Proc. Chem. Soc.*, 389 (1962).
(67) Hoppe, R., Dähne, W., Mattauch, H., and Rödder, K. M., *Angew. Chem. Intern. Ed. Engl.*, **1**, 599 (1962).
(68) Hoppe, R., Mattauch, H., Rödder, K. M., and Dähne, W., *Z. anorg. allgem. Chem.*, **324**, 214 (1963).
(69) Hoppe, R., *Angew. Chem.*, **76**, 455 (1964).
(70) Huston, J. L., Studier, M. H., and Sloth, E. N., *Science*, **143**, 1161 (1964).
(71) Hyman, H. H., "Noble-Gas Compounds," University of Chicago Press, Chicago, Ill., 1963.
(72) Hyman, H. H., *J. Chem. Educ.*, **41**, 174 (1964).
(73) Hyman, H. H., and Quarterman, L. A., "Noble-Gas Compounds," University of Chicago Press, Chicago, Ill., 1963, p. 275.
(74) Ibers, J. A., and Hamilton, W. C., *Science*, **139**, 106 (1963).
(75) Iskraut, A., Taubenest, R., and Schumacher, E., *Chimia*, **18**, 188 (1964).
(76) Israeli, Y. J., *Bull. soc. chim. France*, 6, 1336 (1963).
(77) Israeli, Y. J., *Bull. soc. chim. France* 3, 649 (1964).
(78) Jameson, C. J., and Gutowsky, H. S., *J. Chem. Phys.*, **40**, 1714 (1964).
(79) Jameson, C. J., and Gutowsky, H. S., *J. Chem. Phys.*, **40**, 2285 (1964).
(80) Jaselskis, B., *Science*, **143**, 1324 (1964).
(81) Jaselskis, B., and Vas, S., *J. Am. Chem. Soc.*, **86**, 2078 (1964).
(82) Johnston, W. V., Pilipovich, D., and Sheehan, D. E., "Noble-Gas Compounds," University of Chicago Press, Chicago, Ill., 1963, p. 139.
(83) Jortner, J., Rice, S. A., and Wilson, E. G., *J. Chem. Phys.*, **38**, 2302 (1963).
(84) Jortner, J., Wilson, E. G., and Rice, S. A., *J. Am. Chem. Soc.*, **85**, 814 (1963).
(85) Jortner, J., Wilson, E. G., and Rice, S. A., *J. Am. Chem. Soc.*, **85**, 815 (1963).
(86) Jortner, J., Wilson, E. G., and Rice, S. A., "Noble-Gas Compounds," University of Chicago Press, Chicago, Ill., 1963, p. 358.
(87) Karplus, M., Kern, C. W., and Lazdins, D., *J. Chem. Phys.*, **40**, 3738 (1964).
(88) Kaufman, J. J., *J. Chem. Educ.*, **41**, 183 (1964).
(89) Khutorelskii, V. M., and Shpanskii, V. A., *Dokl. Akad. Nauk SSSR*, **155**, 379 (1964).
(90) King, G. W., and Van Vleck, J. H., *Phys. Rev.*, **56**, 464 (1937).
(91) Kirshenbaum, A. D., and Grosse, A. V., *Science*, **142**, 580 (1963).
(92) Kirshenbaum, A. D., Streng, L. V., Streng, A. G., and Grosse, A. V., *J. Am. Chem. Soc.*, **85**, 360 (1963).
(93) Koch, C. W., and Williamson, S. M., "Noble-Gas Compounds," University of Chicago Press, Chicago, Ill., 1963, p. 181.
(94) Křepinský, J., and Párkányi, C., *Chem. Listy*, **57**, 1233 (1963).
(95) Lavroskaya, G. K., Skurat, V. E., and Tal'roze, V. L., *Dokl. Akad. Nauk SSSR*, **154**, 1160 (1964).
(96) Lazdins, D., Kern, C. W., and Karplus, M., *J. Chem. Phys.*, **39**, 1611 (1963).
(97) Levy, H. A., and Agron, P. A., *J. Am. Chem. Soc.*, **85**, 241 (1963).
(98) Lohr, L. L., Jr., and Lipscomb, W. N., *J. Am. Chem. Soc.*, **85**, 240 (1963).
(99) Lohr, L. L., Jr., and Lipscomb, W. N., "Noble-Gas Compounds," University of Chicago Press, Chicago, Ill., 1963, p. 347.
(100) Lowdin, P. O., "Advances in Chemical Physics," Vol. II, Academic Press, New York, N. Y., 1959, p. 207.
(101) MacKenzie, D. R., and Wiswall, R. H., *Inorg. Chem.*, **2**, 1064 (1963).
(102) MacKenzie, D. R., and Wiswall, R. H., "Noble-Gas Compounds," University of Chicago Press, Chicago, Ill., 1963, p. 81.
(103) Maričić, S., and Veksli, Z., *Croat. Chem. Acta*, **34**, 189 (1962).
(104) Maričić, S., Veksli, Z., Slivnik, J., and Volavšek, B., *Croat. Chem. Acta*, **35**, 77 (1963).
(105) Marsel, J., and Vrščaj, V., *Croat. Chem. Acta*, **34**, 191 (1962).
(106) Mahieux, F., *Compt. rend.*, **257**, 1083 (1963).
(107) Mahieux, F., *Compt. rend.*, **258**, 3497 (1964).
(108) (a) Malm, J. G., Sheft, I., and Chernick, C. L., *J. Am. Chem. Soc.*, **85**, 110 (1963); (b) Malm, J. G., Holt B. D., and Bane, R. W., "Noble-Gas Compounds," University of Chicago Press, Chicago, Ill., 1963, p. 167.
(109) Michels, H. H., "Noble-Gas Compounds," University of Chicago Press, Chicago, Ill., 1963, p. 329.
(110) Milligan, D. E., and Sears, D., *J. Am. Chem. Soc.*, **85**, 823 (1963).
(111) Moody, G. J., and Thomas, J. D. R., "Noble Gases and Their Compounds," Pergamon Press, New York, N. Y., 1964.

(112) Moore, C. E., National Bureau of Standards Circular 467, U. S. Government Printing Office, Washington, D. C.

(113) Morton, J. R., and Falconer, W. E., *J. Chem. Phys.*, **39**, 427 (1963).

(114) Mulliken, R. S., *J. Chem. Phys.*, **7**, 20 (1939).

(115) Mulliken, R. S., *J. Chem. Phys.*, **46**, 497 (1949).

(116) Mulliken, R. S., *J. Am. Chem. Soc.*, **74**, 811 (1952).

(117) Mulliken, R. S., and Pearson, W. B., *Ann. Rev. Phys. Chem.*, **13**, 107 (1962).

(118) Musher, J., *Science*, **141**, 736 (1963).

(119) Neiding, A. B., *Usp. Khim.*, **32**, 501 (1963).

(120) Nesbet, R. K., *Phys. Rev.*, **122**, 1497 (1961).

(121) Nesbet, R. K., *J. Chem. Phys.*, **38**, 1783 (1963).

(122) Noyes, R. M., *J. Am. Chem. Soc.*, **85**, 2202 (1963).

(123) Peacock, R. D., and Holloway, J. H., *Sci. Progr.* (London), **52**, 42 (1964).

(124) Perlow, G. J., and Perlow, M. R., *Rev. Mod. Phys.*, **36**, 353 (1964).

(125) Pimentel, G. C., and Spratley, R. D., *J. Am. Chem. Soc.*, **85**, 826 (1963).

(126) Pimentel, G. C., Spratley, R. D., and Miller, A. R., *Science*, **143**, 674 (1964).

(127) Pitzer, K. S., *Science*, **139**, 414 (1963).

(128) Pollack, G. L., and Broida, H. P., *J. Chem. Phys.*, **38**, 2012 (1963).

(129) Pople, J., *Quart. Rev.* (London), **11**, 273 (1957).

(130) Porter, G., and Smith, M., *Proc. Roy. Soc.* (London), **A261**, 28 (1961).

(131) Pysh, E. S., Jortner, J., and Rice, S. A., *J. Chem. Phys.*, **40**, 2018 (1964).

(132) Reuben, J., Samuel, D., Selig, H., and Shamir, J., *Proc. Chem. Soc.*, 270 (1963).

(133) Roothaan, C. C. J., *Rev. Mod. Phys.*, **23**, 69 (1951).

(134) Roothaan, C. C. J., and Bagus, P. S., "Methods in Computational Physics," Vol. II, Academic Press, New York, N. Y., 1963, p. 47.

(135) Rundle, R. E., *J. Am. Chem. Soc.*, **85**, 112 (1963).

(136) Rutenberg, A. C., *Science*, **140**, 3570 (1963).

(137) Sanderson, R. T., *Inorg. Chem.*, **2**, 660 (1963).

(138) Schumacher, E., and Schaefer, M., *Helv. Chim. Acta*, **47**, 150 (1964).

(139) Selig, H., Claassen, H. H., Chernick, C. L., Malm, J. G., and Huston, J. L., *Science*, **143**, 1322 (1964).

(140) Selig, H., *Science*, **144**, 537 (1964).

(141) Serre, J., *Bull. soc. chim. France*, **1964**, 671.

(142) Sheft, I., and Hyman, H. H., "Noble-Gas Compounds," University of Chicago Press, Chicago, Ill., 1963, p. 68.

(143) Sheft, I., Spittler, T. M., and Martin, F. H., *Science*, **145**, 701 (1964).

(144) Siegel, S., and Gebert, E., "Noble-Gas Compounds" University of Chicago Press, Chicago, Ill., 1963, p. 193.

(145) Siegel, S., and Gebert, E., *J. Am. Chem. Soc.*, **85**, 240 (1963).

(146) Sinanoglu, O., "Advances in Chemical Physics," Vol. VI, Academic Press, New York, N. Y., 1964, p. 315.

(147) Slater, J. C., *Rev. Mod. Phys.*, **25**, 199 (1953).

(148) Slater, J. C., "Quantum Theory of Molecules and Solids," Vol. 1, McGraw-Hill Book Co., Inc., New York, N. Y., 1963, p. 75.

(149) Slivnik, J., Brčič, B., Volavšek, B., Šmalc, A., Frlec, B., Zemljič, R., and Anzur, A., *Croat. Chem. Acta*, **34**, 187 (1962).

(150) Slivnik, J., Brčič, B., Volavšek, B., Marsel, J., Vrščaj, V., Šmalc, A., Frlec, B., and Zemljič, Z., *Croat. Chem. Acta*, **34**, 253 (1962).

(151) Slivnik, J., Volavšek, B., Marsel, J., Vrščaj, V., Šmalc, A.,

(152) Smith, D. F., "Noble-Gas Compounds," University of Chicago Press, Chicago, Ill., 1963, p. 295.

(153) Smith, D. F., *J. Chem. Phys.*, **38**, 270 (1963).

(154) Smith, D. F., *J. Am. Chem. Soc.*, **85**, 816 (1963).

(155) Smith, D. F., "Noble-Gas Compounds," University of Chicago Press, Chicago, Ill., 1963, p. 39.

(156) Smith, D. F., *Science*, **140**, 899 (1963).

(157) Stein, L., and Plurien, P. L., "Noble-Gas Compounds," University of Chicago Press, Chicago, Ill., 1963, p. 144.

(158) Streitwieser, A., Jr., "Molecular Orbital Theory," John Wiley and Sons, Inc., New York, N. Y., 1961.

(159) Streng, A. G., Kirshenbaum, A. D., Streng, L. V., and Grosse, A. V., "Noble-Gas Compounds," University of Chicago Press, Chicago, Ill., 1963, p. 73.

(160) Studier, M. H., and Sloth, E. N., *J. Phys. Chem.*, **67**, 925 (1963).

(161) Svec, H. J., and Flesch, G. D., *Science*, **142**, 954 (1963).

(162) Templeton, D. H., Zalkin, A., Forrester, J. D., and Williamson, S. M., *J. Am. Chem. Soc.*, **85**, 242 (1963).

(163) Templeton, D. H., Zalkin, A., Forrester, J. D., and Williamson, S. M., *J. Am. Chem. Soc.*, **85**, 817 (1963).

(164) Tommila, E., *Suomen Kemistilehti*, **A36**, 209 (1963).

(165) Turner, J. J., and Pimentel, G. C., "Noble-Gas Compounds," University of Chicago Press, Chicago, Ill., 1963, p. 101.

(166) Van Vleck, J. H., and Sherman, A., *Rev. Mod. Phys.*, **7**, 174 (1935).

(167) Wade, C. G., and Waugh, J. S., *J. Chem. Phys.*, **40**, 2063 (1964).

(168) Wahl, A. C., "Analytic Self-Consistent Field Wave Functions and Computed Properties for Homonuclear Diatomic Molecules," Ph.D. Thesis, University of Chicago, 1963.

(169) Ward, R., *J. Chem. Educ.*, **40**, 277 (1963).

(170) Wartenberg, H. V., Sprenger, A., and Taylor, J., *Z. physik. Chem.* (Leipzig), *Bodenstein Festband*, 61 (1931).

(171) Waters, J. H., and Gray, H. B., *J. Am. Chem. Soc.*, **85**, 825 (1963).

(172) Weaver, E. E., Weinstock, B., and Knop, C. P., *J. Am. Chem. Soc.*, **85**, 111 (1963).

(173) Webber, S., Rice, S. A., and Jortner, J., *J. Chem. Phys.*, **41**, 2911 (1964).

(174) Weeks, J. L., Chernick, C. L., and Matheson, M. S., *J. Am. Chem. Soc.*, **84**, 4612 (1962).

(175) Weeks, J. L., and Matheson, M. S., "Noble-Gas Compounds," University of Chicago Press, Chicago, Ill., 1963, p. 89.

(176) Weinstock, B., Weaver, E. E., and Knop, C. P., "Noble-Gas Compounds," University of Chicago Press, Chicago, Ill., 1963, p. 50.

(177) Weinstock, B., Weaver, E. E., and Knop, C. P., presented at 148th National Meeting of the American Chemical Society, Chicago, Ill., Sept. 1964.

(178) Williamson, S. M., and Koch, C. W., *Science*, **139**, 1046 (1963).

(179) Williamson, S. M., and Koch, C. W., "Noble-Gas Compounds," University of Chicago Press, Chicago, Ill., 1963, p. 158.

(180) Wilson, E. B., Decius, J. C., and Cross. P. C., "Molecular Vibrations," McGraw-Hill Book Co., Inc., New York, N. Y., 1955.

(181) Wilson, E. G., Jortner, J., and Rice, S. A., *J. Am. Chem. Soc.*, **85**, 813 (1963).

(182) Yamada, S., *Rev. Phys. Chem. Japan*, **33**, 39 (1963).

(183) Zalkin, A. D., *et al.*, *Science*, **142**, 502 (1963).

Frlec, B., and Zemljič, Z., *Croat. Chem. Acta*, **35**, 81 (1963).